Journal of Geoscience and Environment Protection, 2024, 12, 283-314
https://www.scirp.org/journal/gep
ISSN Online: 2327-4344
ISSN Print: 2327-4336

Interpretation of Geological and Gravity Data from the Bamiléké Plateau (West-Cameroon): Implication for the Understanding of Its Underground Lithotectonic Geometry

Louis Christian Kamgang Chendjou[1*], Jean Victor Kenfack[1], Jules Tcheumenak Kouémo[2], Fidèle Koumetio[3], Armand Kagou Dongmo[1]

[1]Department of Earth Sciences, Faculty of Science, University of Dschang, Dschang, Cameroon
[2]Department of Earth Sciences, Faculty of Sciences, University of Douala, Douala, Cameroon
[3]Department of Physics, Faculty of Sciences, University of Dschang, Dschang, Cameroon
Email: *kamgangc2001@gmail.com

How to cite this paper: Kamgang Chendjou, L. C., Kenfack, J. V., Tcheumenak Kouémo J., Koumetio, F., & Kagou Dongmo, A. (2024). Interpretation of Geological and Gravity Data from the Bamiléké Plateau (West-Cameroon): Implication for the Understanding of Its Underground Lithotectonic Geometry. *Journal of Geoscience and Environment Protection, 12*, 283-314.
https://doi.org/10.4236/gep.2024.129016

Received: August 16, 2024
Accepted: September 26, 2024
Published: September 29, 2024

Abstract

The Bamiléké Plateau represents a key domain in the understanding of the geodynamics associated with the central Cameroon shear. The study aimed to highlight the subsurface architecture of the plateaus basement setting with focus on high potential areas for hydrogeological and mining development projects. To this end, geological field observations were carried out. Since the structures sought were near-surface, a separation approach based on the upward continuation method was applied to the Bouguer anomaly grid. A set of processing techniques, including vertical derivative or *DZ*, analytical signal or *SA* and categorization of gravity signatures, was applied to generate the residual map. The synthesis geological model, obtained from analysis and interpretation of the various transformed maps and 2.5*D* modeling of two gravity profiles *P*1 and *P*2 highlights the following features: 1) intrusions of steep-sided granitic batholiths from Dschang to Bandjoun (profile *P*1), increasing in width from NW (Dschang) to SE (Bandjoun); 2) larger volume batholiths with moderate sides located at Bafang and Bangangté (profile *P*1). These plutonic massifs were weakened by brittle deformation, which favored the emplacement of phonolite or anorthosite dykes within them. The emplacement of these dykes was accompanied by compressional faults with high dip between Dschang and Bandjoun and extensional faults with medium dip between Bafang and Bangangté. These fault zones (trending N85E to N95E) are ideal for hydrogeological investigations in a basement setting, as well as a series of dyke networks that could potentially be preferred zones for the circulation and accumulation

of useful substances. The resulting geological sections *P*1 and *P*2 highlight the influence of granitic intrusions in the geological system of the study area, as well as the structural control associated with the various dyke intrusions. All the models obtained can serve as fundamental references for hydrogeological and mining exploration project on the Bamiléké Plateau.

Keywords

Bamiléké Plateau, Gravity Measurement, Gravity Anomalies, Lineaments

1. Introduction

The Bamiléké Plateau is a vast, very rugged topographical area in western Cameroon, marked by a mountainous landscape dominantly developed on volcanic rocks cover overlaying an ancient bedrock that has undergone major tectonic movements during the Pan-African orogeny (Nguiessi Tchankam et al., 1997; Djouka-Fonkwe et al., 2008; Kwékam et al., 2010, 2015, 2020a, 2020b; Fozing et al., 2021). The current geomorphologic signature of the Bamiléké Plateau can be attributed to relatively recent volcanism, characterized by large volcanic cones such as Mont Bambouto. These volcanic formations, dominantly consist of plateau and flow basalts, are responsible for the imposing Bamiléké Plateau, which ranges in altitudes from 1200 to 1400 m in the study area but culminating at 2,000 m at the summit of Mont Bambouto. The tectonic forces responsible for the plateau's internal geodynamics would have led to the development of the lineaments (faults, shear zones …). Petrographic work of various types including pedologic (Sojien et al., 2018; Mathieu et al., 2012), volcanic (Nkouathio et al., 2008; Ngongang Tchikankou et al., 2020), plutonic and metamorphic petrology as well as structural studies (Njiekak et al., 2008; Kwékam et al., 2010, 2020a; Tcheumenak Kouémo et al., 2014, 2023) have been carried out in this area. Field mapping and structural studies are seriously hindered in this region by the presence of thick lateritic cover from weathering of basalts rock overlaying basement rocks. High-resolution airborne geophysical data have become an indispensable tool for underground geological mapping. Indeed, several studies (O'Leary et al., 1976; Yatabe & Howarth, 1984; Soesilo & Hoppin, 1986) have emphasized the significance of investigating geological lineaments and their role in characterizing structural features such as faults, fractures, fold axes and lithological contacts. The topographic depressions and structural features mentioned earlier may serve as groundwater flow pathways as well as potential mineralization corridors. In Cameroon, several authors have employed geophysics as an investigative tool (Poudjom-Djomani et al., 1996; Kenfack et al., 2011; Koumetio et al., 2012; Ndikum et al., 2017, 2019; Abate Essi et al., 2017, 2018, 2019; Fofie et al., 2019; Ndam Njikam et al., 2022, 2023). The underground of the Bamiléké Plateau through detailed geophysical data is poorly known. This gap in knowledge offers a compelling reason for the scientific community to analyze its subsurface

geological and gravity data.

This study aims to conduct geophysical investigations by applying horizontal gradient, vertical derivative, analytical signal, spectral analysis and 2.5D inversion modeling on gravity data grids in order to develop a lithostructural synthesis model that will help in understanding the underground geometry of the Cameroon Line. It can also be used as a foundational document for hydrogeological or mining investigations in the West Cameroon region.

2. Geological and Tectonic Setting

2.1. The Pan-African Belt in Cameroon

The Pan-African Central African Fold Belt (CAFB) in Cameroon (Penaye et al., 1993; Toteu et al., 2001) is a vast domain limited to the west by the West African Craton and to the south by the Congo Craton. It extends into northeastern Brazil in the province of Borborema, where it forms the Pan-African-Brazilian Belt (Almeida et al., 1981; Brito de Neves et al., 2002) or Sergipano chain (Davison & Santos, 1989). It is considered as the northeastward extension of the Brasiliano belts in Brazil. (Almeida et al., 1981; Brito Neves et al., 2002). The CAFB is connected to the Neoproterozoic Brazilian fold belt (Brito de Neves et al., 2002; Cordani et al., 2003) as demonstrated by Caby et al. (**Figure 1(a)**). It results from a continent-continent collision involving the West African Craton, the Congo and São Francisco Cratons, and the Latea and Saharan Metacratons (Abdelsalam et al., 2002; Liégeois et al., 2003, 2013; Pouclet et al., 2006). The Cameroon domain of the CAFB results from in a continent-continent collision involving the West African Craton, the Saharan Metacratons, the Congo Craton and the active edge of north-central Cameroon showing Archean to Paleoproterozoic legacies (Toteu et al., 2004). According to Njanko et al. (2010), Pan-African tectonic evolution in the Cameroon is characterized by large-scale shear zones, such as the Adamawa Shear Zone (ASZ) and the Tcholliré-Banyo Fault (TBF), which transposed early structures (**Figure 1(b)**). The CAFB is characterized by three units: 1) a cratonic unit in the south (northern part of the Congo Craton); 2) a Pan-African metacratonic unit in the center and 3) a non-metacratonic unit in the north. (Liégeois et al., 2013).

The Pan-African cratonic and non-cratonic units are separated by the Central Cameroon Shear (CCSZ), which forms the transition zone between the two units (Tcheumenak Kouémo, 2018). According to geophysical data from Poudjom Djomani et al. (1995), the crustal thickness contour map shows thickness variation from 14 km to about 45 km, with lower (14 - 20 km) and highest (>20 km) values observed in the central Cameroon and southern Cameroon.

The synthesis of lithostructural data on the CAFB in Cameroon has enabled several authors to propose its subdivision into three lithotectonic domains (Nzenti, 1998; Nzenti et al., 1999; Ngnotué et al., 2000; Toteu et al., 2001; Njanko et al. 2006): a northern, a Central and a southern domain whose limits are defined by Toteu et al. (2001).

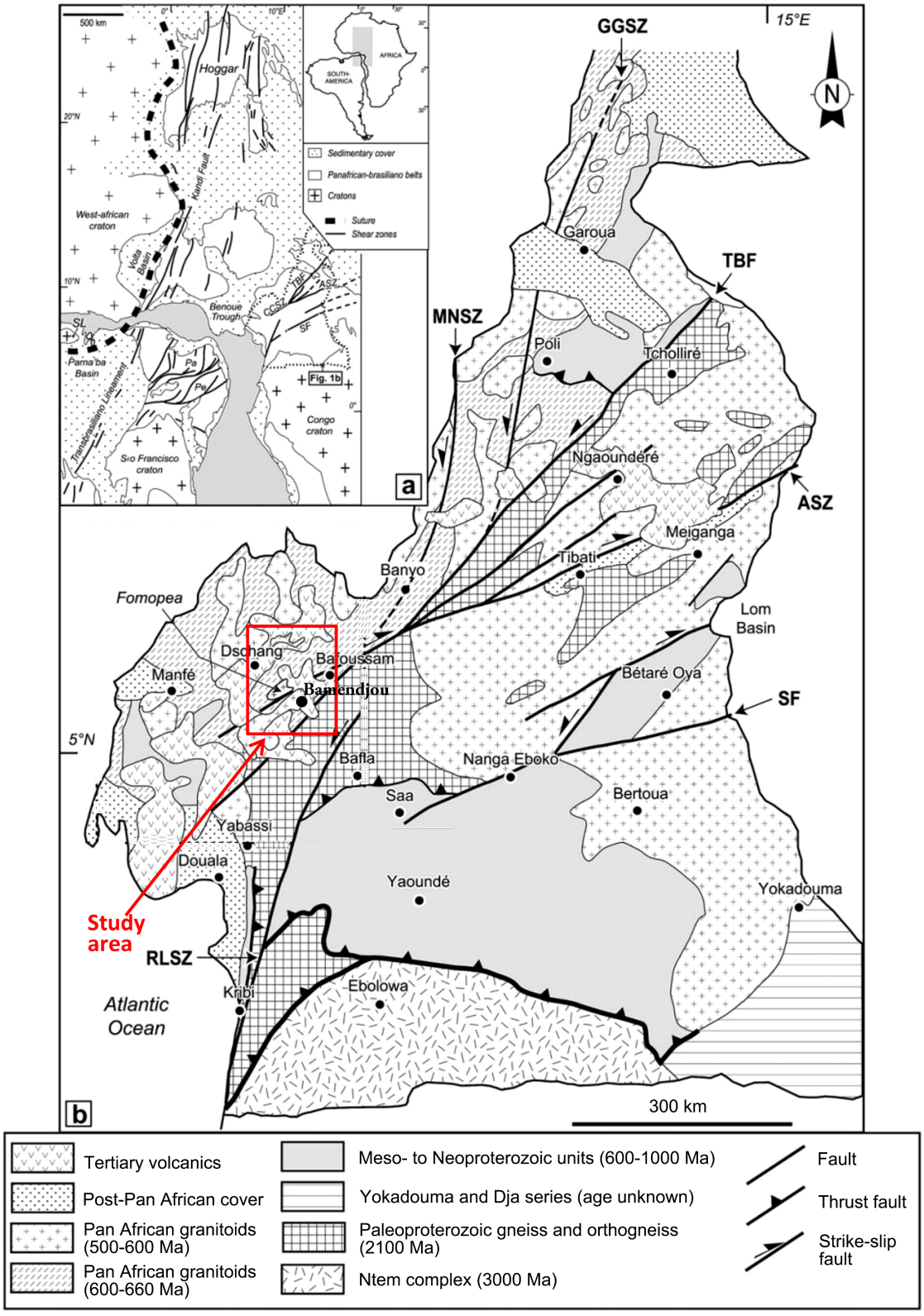

Figure 1. (a) Pre-drift reconstruction. (b) Geological map of Cameroon showing the major lithotectonic domains (after Njanko et al., 2010). ASZ: Adamawa shear zone; CCSZ: Central Cameroon shear zone; GCSZ: Gode'-Gormaya shear zone; MNSZ: Mayo Nolti shear zone; Pa: Patos shear zone; Pe: Pernambuc shear zone; RLSZ: Rocher du Loup shear zone; SF: Sanaga fault; TBF: Tcholliré-Banyo fault.

The Central domain or Adamawa-Yade domain (Toteu et al., 2004), to which the study area belongs, is separated from the Northern domain by the Tcholliré-Banyo shear (CBS) and from the Southern domain by the Sanaga fault (SF). It is characterized by the presence of major strike-slip faults such as the CCSZ (Central Cameroon Shear Zone), which is a N70˚E ductile fault that trends N30E-N50E (Ngako et al., 2003, 2008; Julios et al., 2020; Achu Megnemo et al., 2021; Sobze Yemdji et al., 2023; Tcheumenak Kouémo et al., 2014, 2023, 2024) and the Sanaga Fault (SF), a brittle fault (Toteu et al., 2004). The SF shows a sinistral sense of movement while the CCSZ shows a dextral sense of movement (Ngako et al., 2003, 2008). This domain includes Paleoproterozoic metasediments and orthogneisses intruded by Pan-African syn- to late-tectonic granitoids of crustal or mixed origin (Toteu et al., 2008).

2.2. Geology of the Area

The study area (**Figure 2**) lies between longitudes 10˚00' - 10˚35'E, and latitudes 05˚05' - 05˚45'N and covers an area of 2209 km^2 within the Bamiléké Plateau, which extends between longitudes 09˚44' - 10˚33'E, and latitudes 04˚10' - 05˚56'N in western Cameroon. The Bamiléké Plateau belongs to the West Cameroon Highlands, located both on the N50E branch of the central Cameroon shear zone (CCSZ), whose rocks form the bedrock, and on the Cameroon Volcanic Line (CVL), whose rocks form the volcanic covers. The CVL is a N20E-N30E Cenozoic corridor displaying volcanic rocks extruding the Neoproterozoic Pan-African granito-gneissic basement (Djouka-Fonkwé et al., 2008; Kwékam et al., 2010). The predominant rock types in this area consist mainly of volcanic formations, primarily basalts overlaying on a granite-gneiss bedrock. (Tchouankoué, 1992; Kagou Dongmo et al., 2010) (**Figure 2**). Basalts in the region have two possible origins: They may originate from an asthenospheric source beneath the sub-continental lithosphere (Halliday et al., 1988; Sato et al., 1990), or from amphibole-bearing lithospheric mantle (Marzoli et al., 2000). These volcanic rocks are either subalkaline tholeiite basalt dykes Paleozoic in Dschang, Baham and Bafoussam (420 Ma Tchouankoue et al., 2012, 2014) or Cenozoic to recent magmatic rocks intersecting the basement rocks. The Cenozoic to recent magmatic rocks are considered as intra-plate magmatism developed in a rift context related to the opening of the South Atlantic Ocean (Tchouankoue et al., 2014). These are made up of anorogenic complexes (e.g., Nda Ali massif; Nkogam massif) as well as volcanic cones such as Mt Bambouto, Mt Mbapit (Wandji et al., 2008), Mt Bana (Kuepouo et al., 2006), Mt Bangou (Fosso et al., 2005) along with flow basalts. These rocks exhibit a variety of chemical affinities, including alkaline (Tchuimegnie Ngongang et al., 2015), transitional (Fosso et al., 2005) and tholeiitic (Kuepouo et al., 2006).

The CVL is superposed to the Pan-African Central African Fold Belt (CAFB) in Cameroon (Penaye et al., 1993; Toteu et al., 2001), especially to N30E-N50E branch of the CCSZ. Detailed geological investigations along this CCSZ branch indicate N50E trending syn-tectonic Pan-African granitoids consistent with the

CCSZ NE-SW trend, whose emplacement was controlled by the kinematic evolution of the CCSZ (Njiekak et al., 2008; Djouka-Fonkwé et al., 2008; Fozing et al., 2021; Kwékam et al., 2010, 2020a, 2020b; Tcheumenak Kouémo et al., 2014, 2023). They display dominant calc-alkaline affinity, potassic to shoshonitic (Nguiessi-Tchankam et al., 1997; Tagne-Kamga et al., 2003; Kwékam et al., 2010, 2013) and are generally elongated and aligned in a NE-SW direction, which is consistent with their contemporaneous emplacement within the CCSZ (Ngako, 1999; Tcheumenak Kouémo et al., 2014, 2023; Julios et al., 2020; Achu Megnemo et al., 2021).

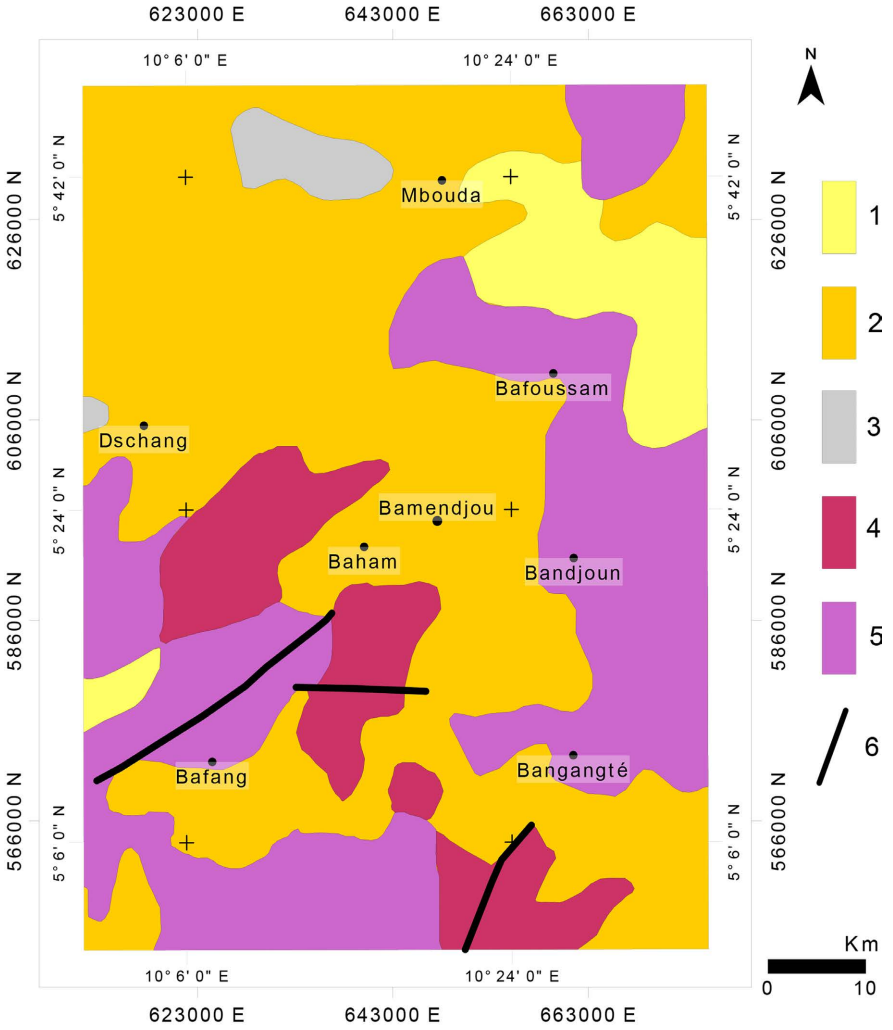

Figure 2. Geological map of the study area (Dumort, 1968, modified by Kwékam et al., 2013. 1: Plio-quaternary volcano-plutonism, Cenozoic; 2: Volcano-plutonism, Cenozoic; 3: Biotite, biotite and amphibole gneiss, Poli-West Cameroon Group; 4: Syn- to late-tectonic granitoids, Neoproterozoic; 5: Pre- to syn-tectonic granitoids, Neoproterozoic; 6: Faults).

The gneissic basement in the area is Paleoproterozoic to Neoproterozoic in age with a reported age of around 2100 Ma (Toteu et al., 2001; Penaye et al., 1993) orthoderived in the Tonga (Tanko Njiosseu et al., 2005), Dschang and Fomopéa (Kwékam et al., 2010, 2020a) to paraderived (in the Kékem locality, Toteu et al.,

2004; Tchaptchet Tchato et al, 2009; Penaye et al., 1993; Tcheumenak Kouémo et al., 2023). Furthermore, it has been metamorphosed to granulite facies (Tchaptchet Tchato et al., 2009; Tcheumenak Kouémo et al., 2023) and contains amphibolitic xenoliths (Fozing et al., 2019, 2021; Tcheumenak Kouémo et al., 2023). These gneiss are remobilized and dislocated along Cameroon mobile zone by the CCSZ (Ngako et al., 2003; Njiekak et al., 2008; Njonfang et al., 2008; Tcheumenak Kouémo et al., 2023). The above Pan-African plutonic and metamorphic basement recorded three main tectonic deformation phases: 1) a D_1 phase dated 622 - 613 Ma (U-Pb on zircon), 2) a D_2 phase dated 613 - 585 (U-Pb on zircon, Kwékam et al., 2010, 2020a, 2020b, 2021) and 3) a D_3 phase dated 580 - 552 Ma (Djouka-Nfonkwé et al., 2008; Tchaptchet Tchato et al., 2009; Kwékam et al., 2020a, 2020b).

3. Data and Processing Methodology

3.1. Data

Gravity data derived from the EGM2008 Earth gravity model, which is provided by the National Geospatial Intelligence Agency were used in this study. The EGM2008 model integrates terrestrial, maritime, airborne gravity data and data derived from satellite altimetry with a resolution of 5 minutes (Pavlis et al., 2008, 2012). It offers excellent spatial resolution for regional studies, addressing the challenge of limited or even absent field data a (Abate Essi et al., 2017, 2019; Zelalem et al., 2018; Maurice et al., 2023).

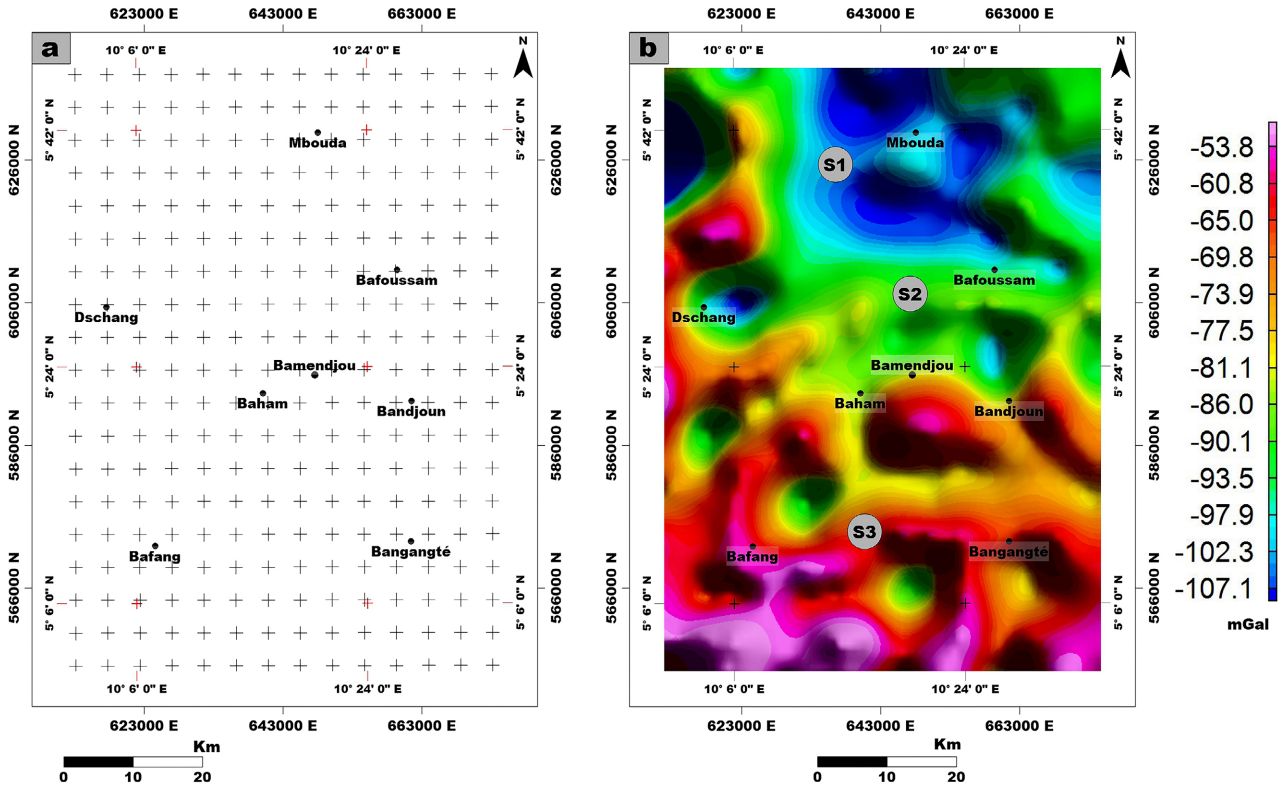

Figure 3. (a) Distribution of gravity points; (b) Bouguer anomaly map.

Bouguer corrections were conducted by BGI and Bouguer anomalies were calculated from spherical harmonic coefficients using FA2BOUG software (Fullea et al., 2008) on an average grid with a resolution of 2.5 minutes by 2.5 minutes. Topographic correction was performed using ETOPO1 digital elevation data (Amante & Eakins, 2008; Balmino et al., 2011). The density reduction for the Bouguer anomaly used was 2.67 g/cm^3. **Figure 3(a)** and **Figure 3(b)** show, respectively, the distribution of gravity measurement points and the Bouguer anomaly map used.

3.2. Processing Methodology

3.2.1. Geological Field Work

The aim of the geological fieldwork carried out in this study is to obtain a set of geological data on which to base the processing and interpretation of the gravity data. Field works were carried out during dry season during which exposures are easily accessed. In the field, petrographic, structural data including foliation, lineation, folds, boudins, and fractures were observed and described. Location of rock types and structural features were done during field studies using a global positioning system. The strikes and dips or plunges of structural features were measured using compass and clinometer. Their geometric analyses allow for classification. These field petrographic and structural data recorded in Dschang, Bafoussam, Bansoa, Bamendjou, Fangam, Fotouni, Fondjomekwet, Bandja, Batié, Kékem, were used for gravimetric maps and cross sections validation.

3.2.2. Gravity, Spectral Analysis, Vertical Derivative

The objective of the gravity analysis conducted in this study includes spectral analysis, vertical derivative calculation, upward continuation, regional - residual separation, analytical signal computation and 2.5D inversion. These processing and interpretation methods aim to extract fundamental structural information to understand the underground geometry of the Bamiléké Plateau and also support hydrogeological and mining investigation projects in this area.

Gravity anomalies can be effectively processed as a spatial series for Fourier synthesis and analysis without affecting the intrinsic appearance of the anomalies (Pal et al., 1979; Reeves, 2005). Spectral analysis does not require a priori knowledge of the geometry or density contrast of the bodies responsible for the observed anomalies. It simply requires the study of spectral energy as a function of wavelength (Saada, 2016; Emishaw et al., 2017; Maurice et al., 2023; Ndam Njikam et al., 2023). Near-surface sources will produce a flatter power spectrum, while deeper sources will give a steeper power spectrum (Pal et al., 1979; Reeves, 2005). Spectral analysis can be performed in 2D or 3D and the depth (h) of an interface can be obtained using Gérard and Griveau (1972) formula given by Equation (1).

$$h = \Delta\left(\mathrm{Log}E\right)/4\pi\Delta\left(n\right) \tag{1}$$

where E represents the energy spectrum; $\Delta\left(\mathrm{Log}E\right)$ is the variation of the logarithm of the energy spectrum in the frequency interval $\Delta\left(n\right)$.

The vertical derivative filter enhances the influence of shallow sources while attenuating the impact of deep sources, thereby concentrating the anomaly and facilitating a more precise delineation of its geometric boundaries (Blakely & Simpson, 1986; Mounir et al., 2012). Specifically, it amplifies shorter wavelengths and individualizes geological bodies in the near subsurface. The nth-order vertical derivative operator is given by Equation (2).

$$\left(O_{DV}\right)_n = \left(-\sqrt{k_x^2 + k_y^2}\right)^n \tag{2}$$

3.2.3. Upward Continuation (UC) and Regional-Residual Separation

The upward continuation (UC) method enables to track the subsurface body's evolution and provides an estimation of its depth extent (Jacobsen, 1987; Koumetio et al., 2012). According to Koumetio et al. (2012), for an upward continuation at a given altitude H, the depth Z of the magnetic or gravimetric anomaly source obtained is greater than or equal to half of H (Equation (3)).

$$Z \geq H/2 \tag{3}$$

UC is widely employed in various studies as a regional-residual separation method (Zelalem et al., 2018; Arsène et al., 2019; Maurice et al., 2023). Here, it is used to calculate a regional grid by simply extending it upwards to an altitude (H) set by the geophysicist given Equation (4) as follows:

$$\text{Residual field} = \text{Field of origin} - \text{Regional field} \tag{4}$$

3.2.4. Analytical Signal (AS)

The analytical signal method is highly effective in highlighting intrusions or contacts zones. Numerous studies employ this approach not only for structural interpretation, but also to highlight zones of formation under cover. (Arsène et al., 2019; Maurice et al., 2023). It is a function of the horizontal (along x and along y) and the vertical (along z) derivative given by Equation (5):

$$ASA(x,y) = \sqrt{\left(\frac{\partial f(x,y)}{\partial x}\right)^2 + \left(\frac{\partial f(x,y)}{\partial y}\right)^2 + \left(\frac{\partial f(x,y)}{\partial z}\right)^2} \tag{5}$$

3.2.5. 2.5D Inversion

2.5D modeling consists in searching for a subsurface model that best reproduces the anomaly observed on the surface, i.e., a model taken in the sense of a particular discrete distribution of densities, magnetizations or resistivities at depth (Kpirgbéne et al., 2016). In the context of gravity anomalies, 2.5D modeling involves restricting the infinite field of potential models to a finite, or at least bounded, set of geologically acceptable models. The practice of interpreting potential data using modeling software has a long history, with GM-SYS, developed by Geosoft, emerging as one of the most widely employed software packages for such tasks (Emishaw et al., 2017; Zelalem et al., 2018; Arsène et al., 2019; Abate Essi et al., 2019; Ndam Njikam et al., 2023) GM-SYS provides an optimal platform for 2.5D modeling.

The approaches used by GM-SYS to calculate the response of a gravity model are based on the methods of Talwani et al. (1959) and Talwani and Heirtzler (1964), and utilize the algorithms as described by Won and Bevis (1987). Typically, an initially infinite polygon with "n" sides (2*D* model) is iteratively adjusted to match the collected data (smoothing). In the method developed by Talwani et al. (1959) by Talwani & Heirtzler (1964), the lateral extension of the polygon is no longer infinite and the model is said to be two-and-a-half-dimensional (2.5*D*). The mathematical expression for a 2.5*D* polygon was developed by Shuey & Pasquale (1973) (Equation (6)). To adapt the model's theoretical curve to that of the measured data, the polygon geometry is progressively modified, either manually or by successive iterations (semi-automatic mode) using the non-linear least squares method (Powell, 1965).

$$B_{y(n)} = -2Jj_y \sum \left(\tan^{-1} \frac{u_{i+1} + Y}{w_i R_{i+1}} - \tan^{-1} \frac{u_i Y}{w_i R_i} \right) \tag{6}$$

where x is the profile axis, z the vertical axis and Y the axis orthogonal to the other two; J is the magnetization of the body under consideration; u and w are the frequencies of the source signal.

$$R_i = \sqrt{\left(u_i^2 + w_i^2 + Y^2\right)}; \quad r_{i+1} = \sqrt{\left(u_{i+1}^2 + w_i^2\right)}; \quad w_i = -\sin \varnothing_i x_i + \cos \varnothing_i x_{i+1} \quad \text{et}$$
$$u_i = \cos \varnothing_i x_{i+1} + \sin \varnothing_i z_i .$$

To model the subsurface of the study area, two cross-section *P*1 and *P*2 intersecting the maximum geological structures (with orientations ranging from NNE-SSW, NE-SW to ESE-WNW) were chosen. Furthermore, we chosed profiles *P*1 and *P*2 to intersect the CVL and within the Bamendjou zone, aligning with the primary geological facies already identified through previous observations.

Since the investigated features of interest were near-surface, a regional-residual separation approach was applied to the Bouguer anomaly data using the up-dip separation method, coupled with spectral analysis. The residual data from the above highlights anomalies between the surface and an average maximum depth reference for discontinuities studies. A series of processing operations were then applied to the residual grid (vertical derivative, analytical signal or SA and categorisation of gravity signatures). Analysis of the vertical derivative map reveals structural pattern that may indicate faults directions and depths affecting the underground geological organization in the study area. Finally, results of gravitric investigations, the categorisation of the gravity signatures and field observations enabled to draw a geological synthesis model of the Bamiléké Plateau.

4. Results and Discussion

4.1. Geological Field Work

The geological data collected during fieldwork primarily comprise petrographic and structural information, as depicted in **Figure 4**. Generally, the study area is characterized by an extensive soil cover, which can be attributed to the significant

weathering of the local geological formations. This alteration is justified not only by the study area location in the Bamiléké Plateau, but also by its geomorphology, which accentuates the phenomenon of weathering (Figure 4(a)). Several factors have contributed to soil formation, including geological nature of the bedrock, to which relief and topography are linked.

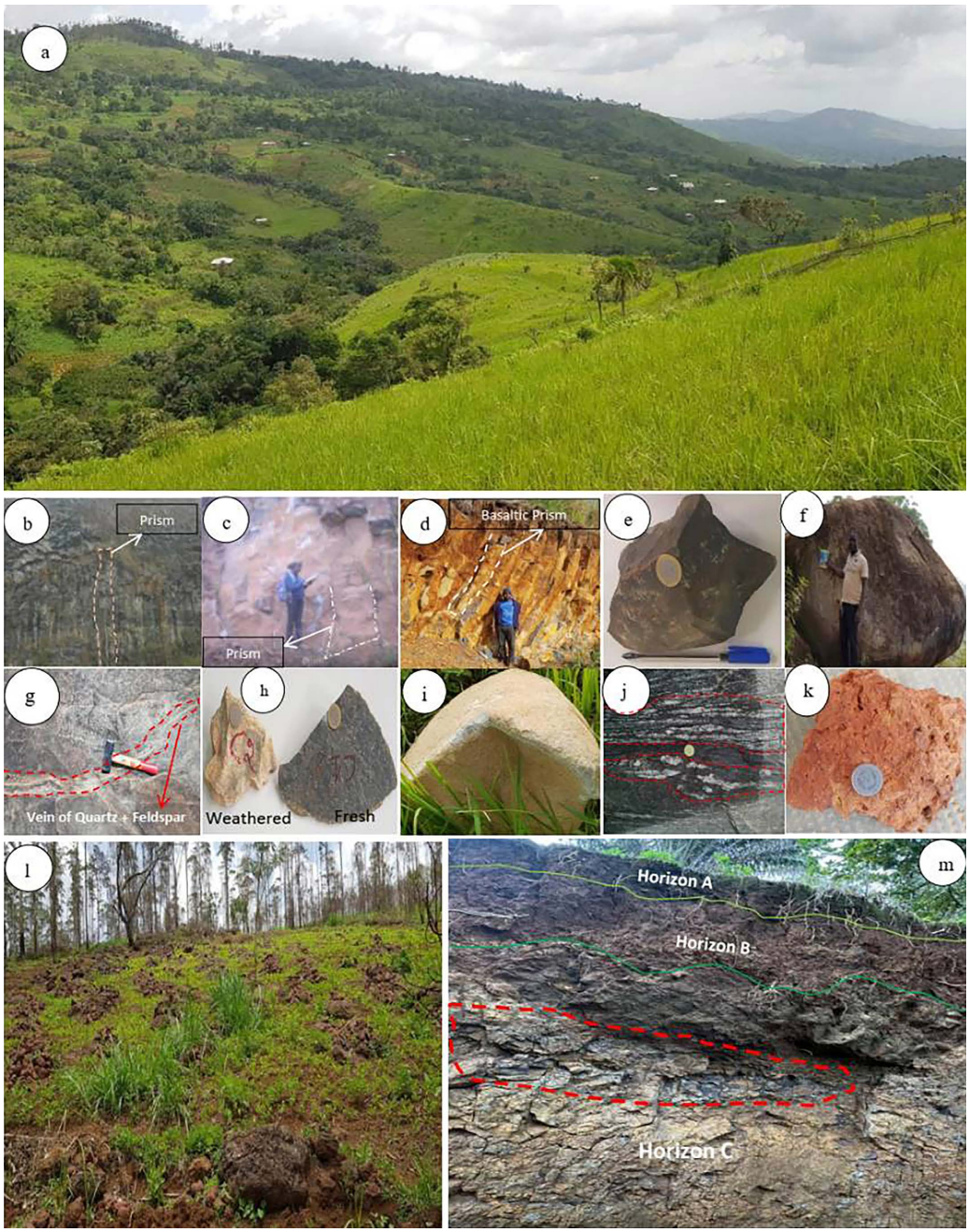

Figure 4. (a) Bamiléké plateau panoramic view; (b) Basaltic prism in Fangam; (c) Basaltic prism in Fotouni; (d) Basaltic prism in Bamendjou; (e) Fresh basalt sample; (f) Fresh granite outcrop in Bansoa; (g) Vein of quartz-feldspar in granite outcrop; (h) Weathered/fresh basalt samples; (i) Fresh granite sample; (j) Boudinated clear band of gneiss; (k) Lateritic sample; (l) Lateritic cover; (m) Example of soil profile observed in trenche representing the different horizons A, B and C.

Recent basalts are limited to a small geographic area, specifically in Baleng and Foumbot. These basalts are scoriaceous in nature, appearing dark gray to black, often with bubbly and very glassy texture sometimes rich in olivine, but without feldspars, with numerous pyroclastic products: boulders, bombs, lapillis and pozzolans, all of which can form real formations and are characteristic of Vulcan-type eruptions.

In contrast, ancient basalts are Hawaiian-type flows and represent the most widespread dynamism in the study area (**Figures 4(b)-(d)** and **Figure 4(e)**). These basalts dominantly composed of olivine and pyroxene which outcrop as blocks and prisms of up to 30 m height in quarries in the localities of Bafoussam, Baham, Bamendjou, Bandjoun, Bangangté, Dschang, Fangam, Fotouni and Mbouda (**Figure 4(b)**, **Figure 4(c)** and **Figure 4(d)**). The basalts encountered are dark in color with a reddish-yellow weathering patina. They mostly display microlitic or porphyritic microlitic texture, as illustrated in **Figure 4(e)**. However, some few volcanic rocks of basaltic composition displaying pyroclastic textures, including pozzolans, found in Bafoussam (Baleng). These pyroclastic matirials appear in shades ranging from black to brown and consist predominantly of amorphous volcanic glass.

The basement geological formations in the study area are plutono-metamorphic rocks including granites and gneisses. Biotite granite, the most common type, dominantly outcrop in the southern and central domaines of the study area, where they occur as blocks and slabs on slopes and hilltops in Dschang, Batié, Bansoa, Bamendjou and Bafoussam. It is very often altered but recognizable by its grainy structure (**Figures 4(f)-(h)** and **Figure 4(i)**). This granite is very often rich in alkali feldspar megacrysts at Dschang, Fomopéa, Bandja, Batié and Bafoussam and also consist mainly of plagioclase, quartz and biotite. The least altered granites are found near riverbeds, where they are covered with patina. They are very often cross cut by quartz-feldspar veins (**Figure 4(g)**), which are highly altered (**Figure 4(h)**) and transform into clay minerals (**Figure 4(i)**). Quartz appears heteromorphic and the whole is fairly leucocratic and homogeneous. However, basement gneisses outcrop episodically as flagstones consisting of biotite gneiss (Dschang, Mbouda, etc.). Two-mica gneisses, characterized by their leucocratic nature, are exceptionally hard and exhibit patchy peeling along the dames. In addition, sillimanite and kyanite garnet gneisses featuring alternating light and dark bands outcrop in Kékem with, the light bands displaying size variation from a millimeter to 30 cm. dark bands rich in biotite and garnet and vary in size from 2 mm to 1 m. The clear bands are sometimes stretched and boudinateded (**Figure 4(j)**). The paragneiss and orthogneiss are crushed, along a shear zone to form mylonites that outcrop as a corridor between Kékem and Bafoussam. Overall, the granito-gneissic basement rocks in the study area display pockets of rocks with embrittlement facies, as well as veins of aplites and pegmatites with very large quartz phenocrysts. This ancient granite-gneissic basement is covered, in the study area, mainly by ancient and recent volcanic formations.

Figure 5. Field observations in metamorphic (a, b, c, e, f, g, h) and plutonic (d) rocks from the Bamiléké Plateau. (a) Metamorphic S_1/S_2 foliation in orthogneiss from Dschang area, showing F_2 fold resulting from the transposition of S_1 into S_2 during D_2 deformation phase. (b) F_2 fold details and transposition phenomenon, redrawn from (a). (a)-(c) NE-SW foliation in paragneiss from Kékem. Note also the symmetric bodins display by clear bands and the NE-SW sinistral shear plane shown by a fracture d) NNW-SSE to NNE-SSW mamatic foliation from Batié synkinematic granite. (e)-(f) NE-SW mylonitic foliation indicates by preferred orientation of garnet (e) and quartz (f) crystals. Note also the dextral rotation display by garnet and quartz crystals. (g) Symmetric and asymmetric bodins in mylonites from Fondjomekwet. Note also the dextral sens of motion displays by the asymmetric boudin. (h) NNW-SSE sinistral shear plane display by a shear facture in mylonites from Fondjomekwet. Note also the dextral sens of motion displays by the asymmetric boudin.

Almost the entire basaltic formation covers in the study area is dominated by cuirasses and lateritic blankets. These lateritic covers are also observed above the plutono-metamorphic basement (Figure 4(k) and Figure 4(l)) and indicate intense weathering, often resulting from lateritic soil profiles that reach 10 to 20 meters heights. They cover large areas of several hundred km^2.

The primary driving factor behind the lateritic alteration of volcanic rocks in the Western Highlands of Cameroon is the prevailing climatic conditions (Figure 4(k)) in the Western Highlands of Cameroon. These cuirasses are composed of goethite, hematite, aluminum hydroxide, iron oxy-hydroxide (goethite and hematite), gibbsite, kaolinite and quartz.

The tectonic structures identified in the granitic-gneissic basement include foliation, folds, boudins, shear planes, fractures and veins. The foliation is gneissic (Figure 5(a), Figure 5(b)), magmatic (Figure 5(c)) or mylonitic (Figure 5(d), Figure 5(e)). The gneissic foliation is characterized by alternating light and dark bands-oriented NNW-SSE (syn-D_1), transposed N-S to NNE-SSW (syn-D_2) and transposed NE-SW (syn-D_3). Magmatic foliation primarily manifests as the preferential alignment of alkali feldspar phenocrysts (Figure 5(b)) oriented in a NNE-SSW (N30E) to NE-SW (N50E) direction (syn-D_2). In mylonites, foliation is shown by the preferential orientation of quartz, biotite and garnet crystals in light and dark bands. N-S to NNE-SSW directions (syn-D_2) transposed to NE-SW (Syn-D_3) are observed.

The folds are very often anisopaque with NE-SW trending axes, displaying gentle to moderately toward the SW or NE. Boudins are materialized by the constriction of metamorphic foliation or clear bands (Figure 5(c)).

Shear planes are sinistral N-S (syn-D_2, Figure 5(d)) or dextral NE-SW (syn-D_3, Figure 5(e)), materialized by ductile transposition of foliation or veins.

Fractures (Figure 5(f)) and quartz veins are observed in both gneiss and granite in which they display NW-SE (N120E-N150E) or NE-SW (N50E-N70E) direction.

4.2. Bouguer Anomaly Map and Regional-Residual Separation

Based on the data provided by the BGI (Figure 3(a)), the Bouguer anomaly map (Figure 3(b)) was drawn up using minimum curvature as the interpolation method for a sampling step of 0.01 degrees (i.e., approx. 1.1 km). This map shows anomaly amplitudes ranging from −107.1 to −53.8 mGal. The relief of the anomalies appears fairly smooth, uniform and above all undisturbed, due to the resolution of the gravity data used (approx. 4 km × 4 km). This resolution has a major influence on local anomalies, which are generally small in extent, as they are masked by density contrasts linked to regional structures or formations. The Bouguer anomaly map reveals the presence of three distinct anomaly domains (Figure 3(b)): 1) the *S*1 domain exhibits negative or low-gravity anomaly, which may correspond to areas where basaltic flows have been observed in the field; 2) the *S*2 domain represents a medium-gravity anomaly zone, which extends across the entire gravity model and likely corresponds to the dominant basement structure

within the study area; 3) the *S*3 domain shows positive anomaly values, which could potentially be associated with either intrusive features or ancient sedimentary deposits.

In order to determine the mean maximum depth associated with the anomalies and establish distinct depth domains, a 2*D* radial spectrum was applied to the Bouguer anomaly grid. The analysis of the resulting spectrum (Figure 6) reveals average depth slices corresponding to three information domains. According to the spectrum analysis, the average maximum depth of deep sources (*SP*) is estimated to be 7.948 km, that of intermediate sources (*SI*) is approximately 2.9 km and that of near-surface sources (*SPS*) is approximately 0.99 km. This estimation suggests the maximum depth reached by gravity signals is approximately 8 km. To eliminate the influence of very deep anomaly sources, a residual grid was calculated using the upward continuation separation approach described in the methodology.

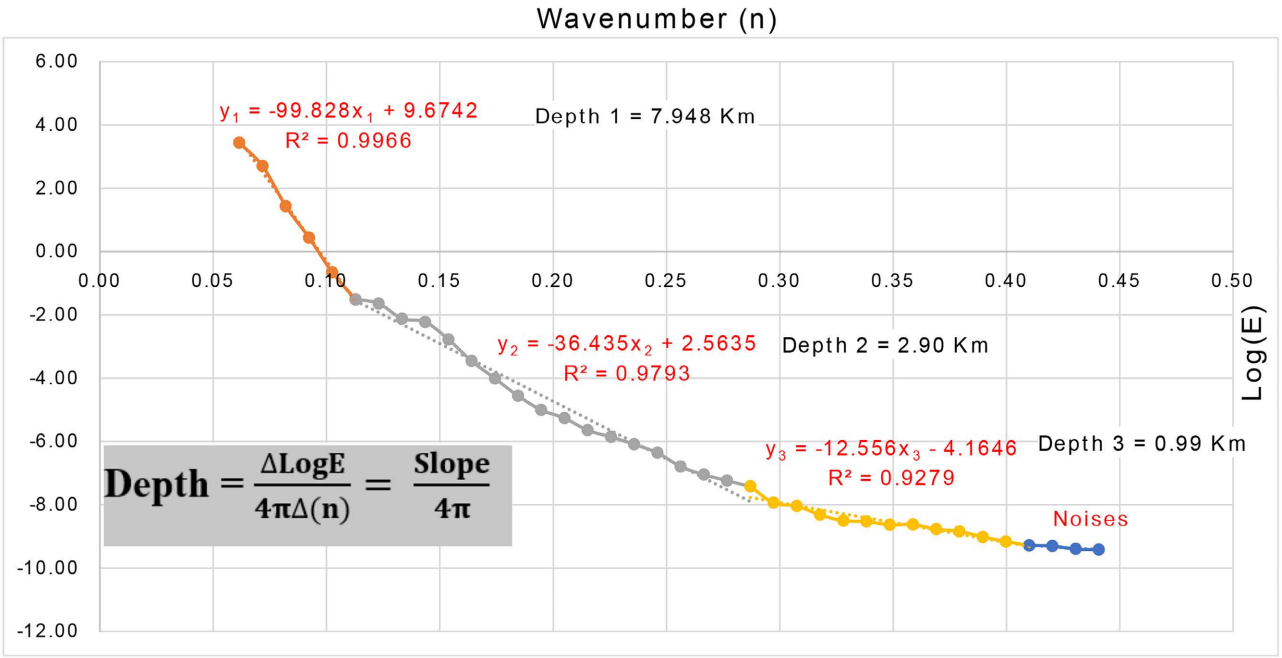

Figure 6. Power spectrum associated with the Bouguer anomaly grid.

4.3. Analysis of the Residual, Vertical Derivative and Analytical Signal Map

To obtain the residual, an upward continuation of the Bouguer was made at an attitude of 8 km, and the residual grid was then calculated as the difference between the regional (map extended to 8 km) and the Bouguer anomaly map. The spectral analysis shows that the geological structures contributing to the Bouguer anomaly evaluation extend to a depth (*H*) of approximately 8 kilometers, our objective is to analyze the effects of structures located at a depth less than or equal to *H*/2, i.e. around 4 km. Unlike the Bouguer grid, where anomaly amplitudes range from −107.1 to −53.8 nT, the residual (Figure 7) shows that they range from −18.8

to −16.6 nT. This shows that separation has been achieved and that the influence of anomaly sources at depths greater than around 4 km has been filtered out. The organization of the anomalies has also been modified, as here the anomalies are much more disturbed. The negative anomalies in the *S*1 domain, previously interpreted as corresponding to basaltic flow zones, are very discontinuous and more widespread in the residual model. In fact, these basaltic flows were observed during the geological campaign at several sites in the study area.

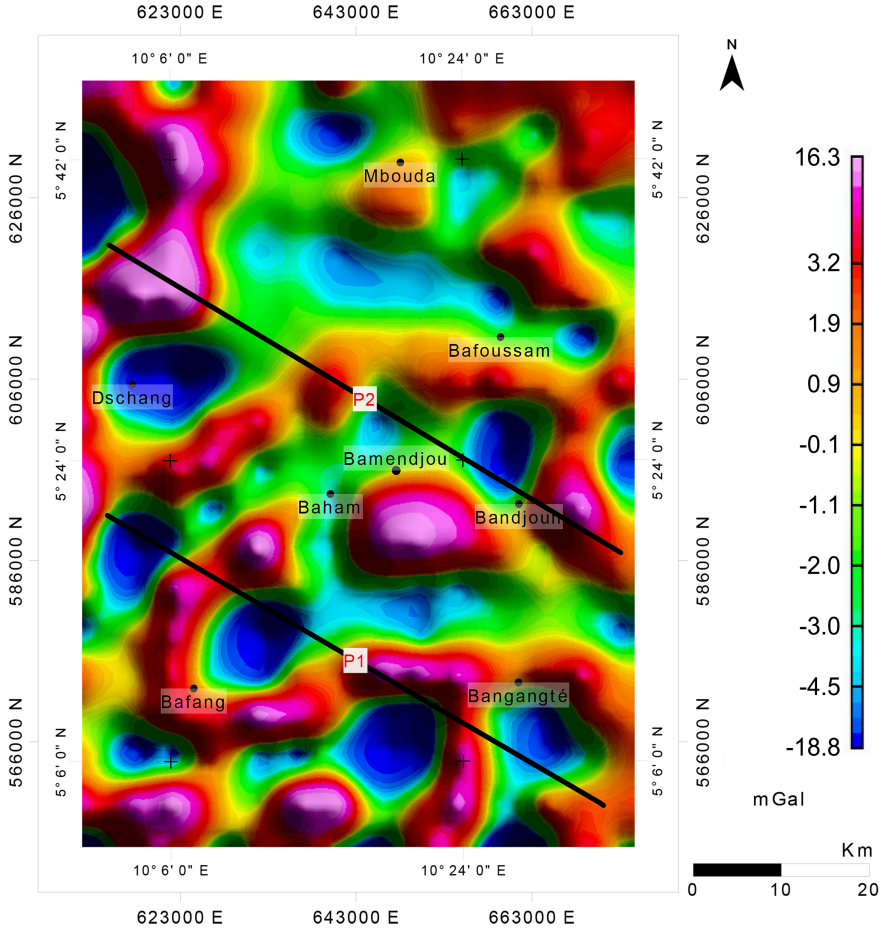

Figure 7. Residual anomaly map (*P*1 and *P*2 are the profiles used for 2.5*D* modeling).

The mean anomalies, depicted in green, and associated with the *S*2 domain on the Bouguer grid extend over the entire residual model. This extensive presence within the study area reaffirms our earlier interpretation that this domain corresponds to the dominant basement. However, in contrast, the *S*3 domain of the Bouguer grid no longer exhibits continuity in the residual model. This observation arises from the fact that the intrusive bodies observed in the *S*3 zone are characterized by significantly higher density values compared to the average density of deep, extensive geological structures. The positive anomalies of this domain are much more rectilinear with orientations mainly E-W to NE-SW but also N-S (**Figure 8**) that may correspond to dolerite or basalt dykes observed in the field that took

advantage of N-S zones of weakness developed during the D_2 deformation phase (Njanko et al., 2010, Tcheumenak Kouémo et al., 2014, 2023), which thus corroborates the work of many authors (Nguiessi-Tchamkam et al., 1997; Tagne-Kamga et al., 2003; Njanko et al., 2006; Djouka-Fonkwé et al., 2008; Kwekam et al., 2010, 2013).

To ensure that these rectilinear anomalies corresponded to the dykes, a vertical derivative filter was applied to the residual grid (**Figure 7**). The vertical derivative was used to determine the directions of the structures and, based on field observations, the faults and their kinematics were illustrated on the derived model (**Figure 8**) obtained. The model thus allows us to better define the limits of these rectilinear anomalies, demonstrating at the same time that they are near-surface, and confirming the geological results obtained in the study area with regard to fault delineation.

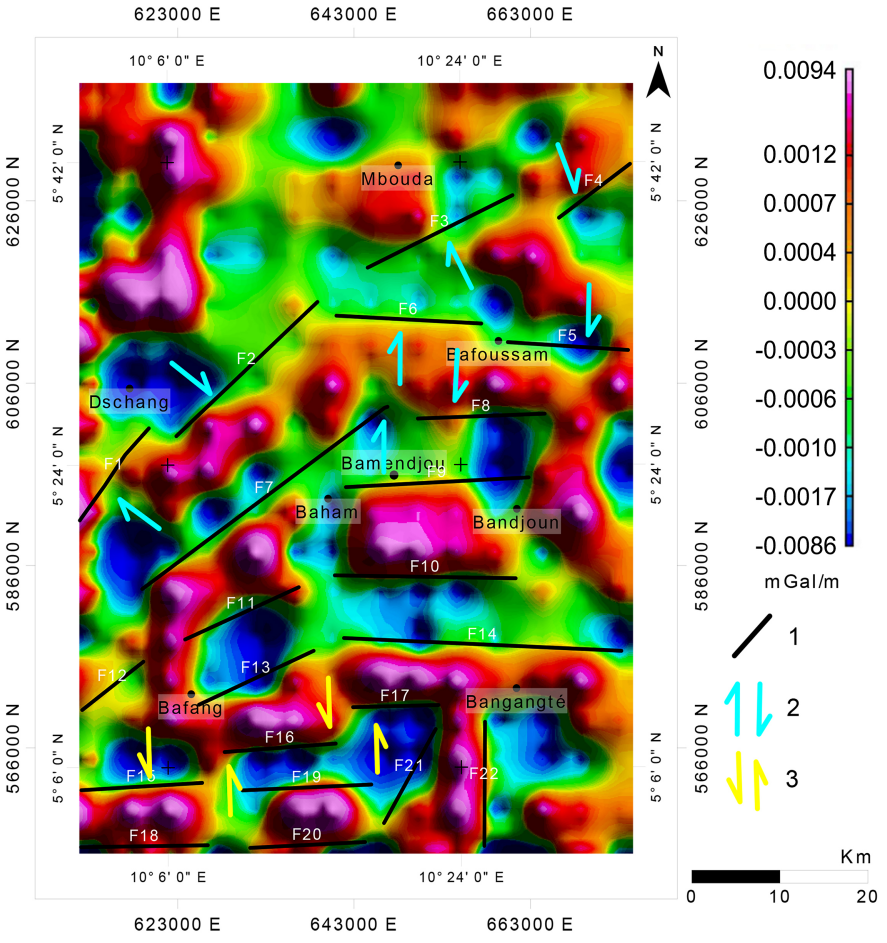

Figure 8. Residual vertical derivative map (1: Faults; 2: Dextral movement; 3: sinistral movement).

Figure 8 and **Table 1** show 22 faults (numbered *F*1 to *F*22) and their kinematics, ranging in length from 8.74 km to 34.27 km, with an average length of 16.14 km. The cumulative length of the mapped faults is 355.16 km, with the longest fault in the center of the map running N30˚E. Among these faults, *F*1, *F*2, *F*7 and *F*11 have

already been highlighted in several studies. (Dumort, 1968; Ngako et al., 2003; Toteu et al., 2008; Njanko et al., 2010; Kwékam et al., 2010; 2013; Tcheumenak Kouémo et al., 2014, Tcheumenak Kouémo, 2018; Tchuimegnie Ngongang et al., 2015; Blandine et al, 2022).

The analysis of these anomalies within the derived model indicates that they are controlled by faults defining a dextral kinematics in the center (at Bamendjou) and north of Bamendjou, and a sinistral kinematics south of Bamendjou (**Figure 8**). These faults, whose major directions vary from N85E (ENE-WSW) to N95E (ESE-WNW) (**Figure 8**, **Figure 10**), these fault patterns correspond to a set of dextral and sinistral structures characteristic of the central Cameroon shear corridor, to which the study area is affiliated (Ngako et al., 2003; Tchameni et al., 2006; Toteu et al., 2008; Ngako et al., 2008; Kwékam et al., 2010). From a hydrogeological perspective, the fault networks highlighted in this model could potentially represent ideal zones for the exploration of fracture aquifers.

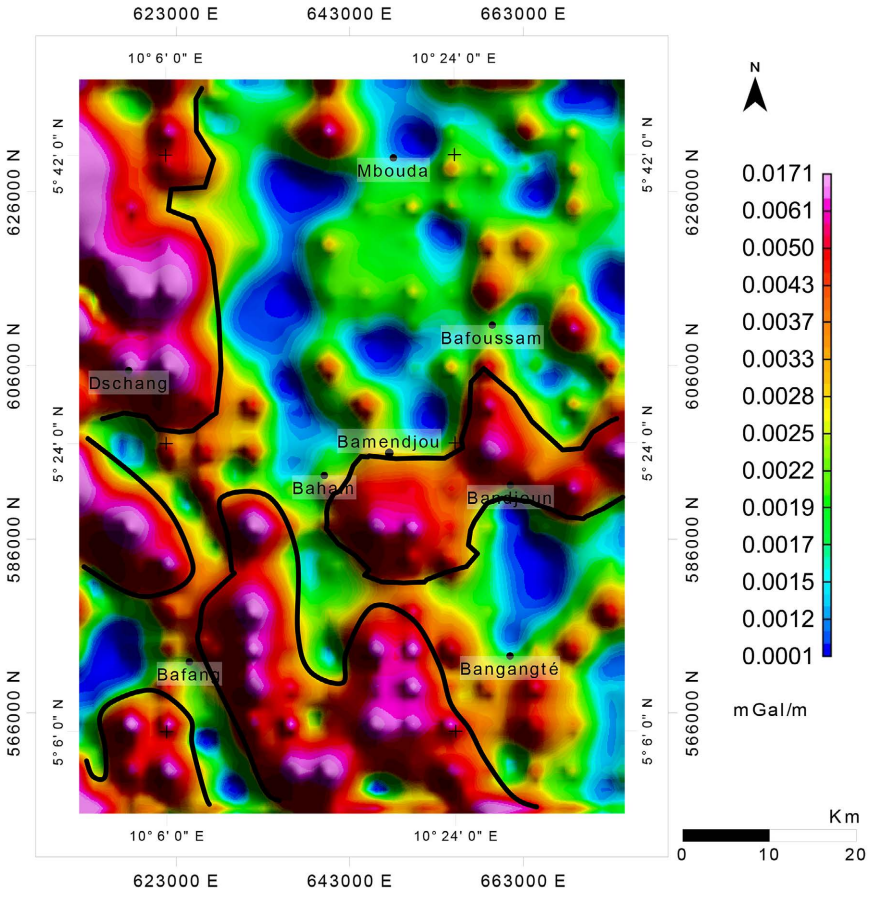

Figure 9. Analytical signal map highlighting anomalies associated with granitic intrusions (thick black lines correspond to lithological contours).

To highlight granitic intrusions areas whose gravity signal is masked by near-surface sources, an analytical signal filter was applied to the residual grid. The resulting map (**Figure 9**) enhances the relief of anomalies corresponding to granitic

intrusions whose boundaries correspond to the lithological contacts that can be represented (thick black lines on **Figure 9**). This outcome effectively highlights the anomalies associated with granitic intrusions within the study area, with the most pronounced occurrences located in the southern, western (Dschang), and central regions near Bamendjou, Baham, and Bandjoun, as confirmed through field observations.

5. Interpretation of the Transformed Maps for the Elaboration of a Geological Synthesis Model and 2.5*D* Modeling

Based on the various analyses carried out to date including residual map, vertical derivative and analytical signal analysis and the categorization of gravity signatures according to the gravity map used, a geological synthesis model has been developed (**Figure 10**). This model shows a predominantly granito-gneissic basement with a predominance of gneiss covered mainly by volcanic formations. This is witnessed in the field by dominant lateritic covers resulting from weathering of basalts (**Figures 4(b)-(d)**, **Figure 4(l)**, **Figure 4(m)**) (Nkouathio et al., 2008; Zangmo Tefogoum et al., 2019; Ngongang Tchikankou et al., 2020; Tchuimegnie Ngongang et al., 2015) and granito-gneissic basement rocks (Djouka-Fonkwé et al., 2008; Njiekak et al., 2008; Kwekam et al., 2010, 2015, 2020a, 2020b; Tchouankoue et al., 2012, 2014; Fozing et al., 2021). Within this basement, numerous deformations have played a significant role in shaping the geological architecture of the study area. These deformations are characterized by both dextral movements, observed in the central and northern regions of Bamendjou, and sinistral movements, identified to the south of Bamendjou (Tcheumenak Kouémo et al., 2014, 2023). The occurrence of dyke indicated by 2.5*D* model of **Figure 12** and **Figure 13** is evidence in the field by the anorthosic dyke (Ziada Tabengo et al., 2022) Nzindeng phonolites (Nkouathio et al., 2008; Njanko et al., 2020) respectively. Consequently, the geological model obtained exhibits a complex and chaotic appearance. Consequently, the geological model obtained exhibits a complex and chaotic appearance.

Figure 10 evidences an E-W volcanic dyke in Bamedjou as shown by **Figures 4(b)-(d)**. Geoelectric data of the area from unpublished works by Kamgang Chendjou show that this dyke underground water reservoir into two most productive reservoirs including the one to the north and the other to the south of this intrusion within fractured and weathered basalts.

Table 1 shows the directions and approximate lengths of all geological lineaments interpreted as deep faults in the Bamiléké Plateau.

Figure 11 shows the orientation (E-W to NNW-SSE) of these anomalies, which corresponds. to the descriptions given in numerous studies of granitic formations in the study area (Dumort, 1968; Ngako et al., 2003, 2008; Toteu et al., 2008; Njanko et al., 2010; Kwékam et al., 2010; 2013; Tcheumenak Kouémo et al., 2014, Tcheumenak Kouémo, 2018; Tchuimegnie Ngongang et al., 2015; Blandine et al, 2022).

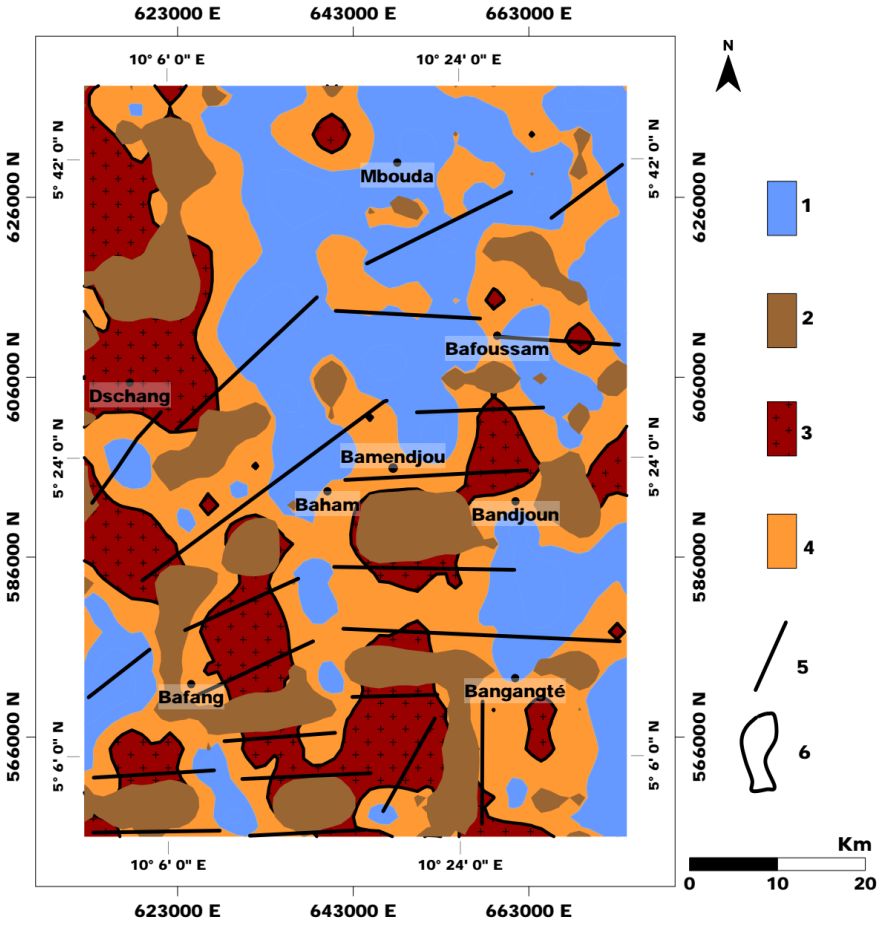

Figure 10. Geological synthesis model (1: Volcanic formations; 2: Dykes; 3: Granitic intrusions; 4: Gneissic bedrock; 5: Faults; 6: Lithological contours).

Table 1. Characteristics of the various deep faults on the Bamiléké Plateau.

Faults	Fault trends	Approximate lengths (km)
F1	N38E	12.81
F2	N48E	21.75
F3	N64E	18.26
F4	N54E	9.99
F5	N94E	13.67
F6	N93E	16.46
F7	N54E	34.27
F8	N88E	14.41
F9	N87E	20.76
F10	N91E	20.52
F11	N66E	14.11
F12	N53E	8.74

Continued

F13	N66E	14.28
F14	N93E	31.51
F15	N87E	13.73
F16	N86E	12.64
F17	N89E	9.7
F18	N89E	14.4
F19	N88E	14.63
F20	N87E	13.05
F21	N30E	11.87
F22	N180E	13.61

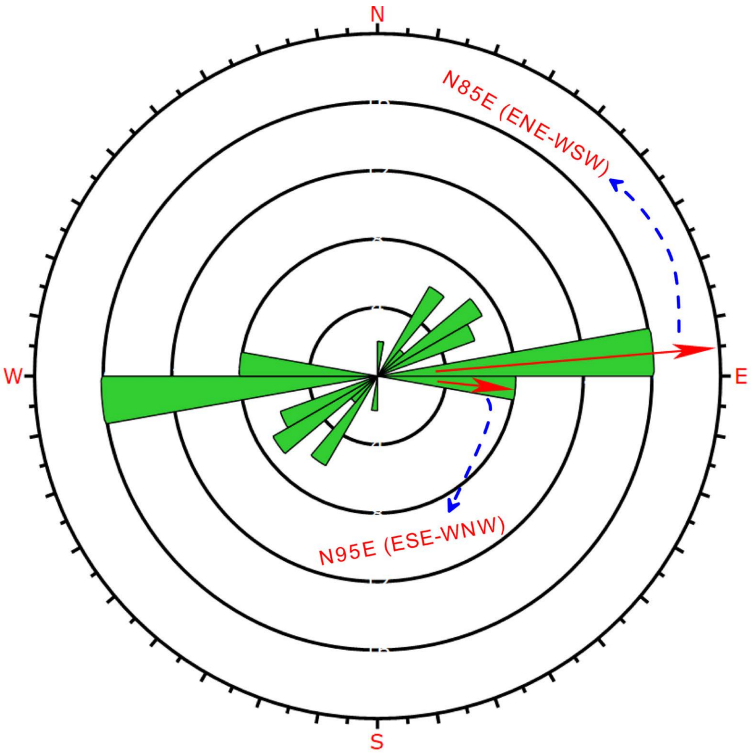

Figure 11. Directional rosette of fault orientations.

The granitic formations are cut across by dykes whose kinematics show that their emplacement was favored by the tectonic activities that affected the basement. To study the vertical architecture of geological structures and formations in the study area, 2.5*D* inversion modeling of two gravity profiles *P*1 and *P*2 traced from the residual map (**Figure 7**) was carried out. The geological sections resulting from this modeling (**Figure 12** and **Figure 13**) show the influence of granitic intrusions in the geological system of the study area, as well as the structural control associated with the various dyke intrusions.

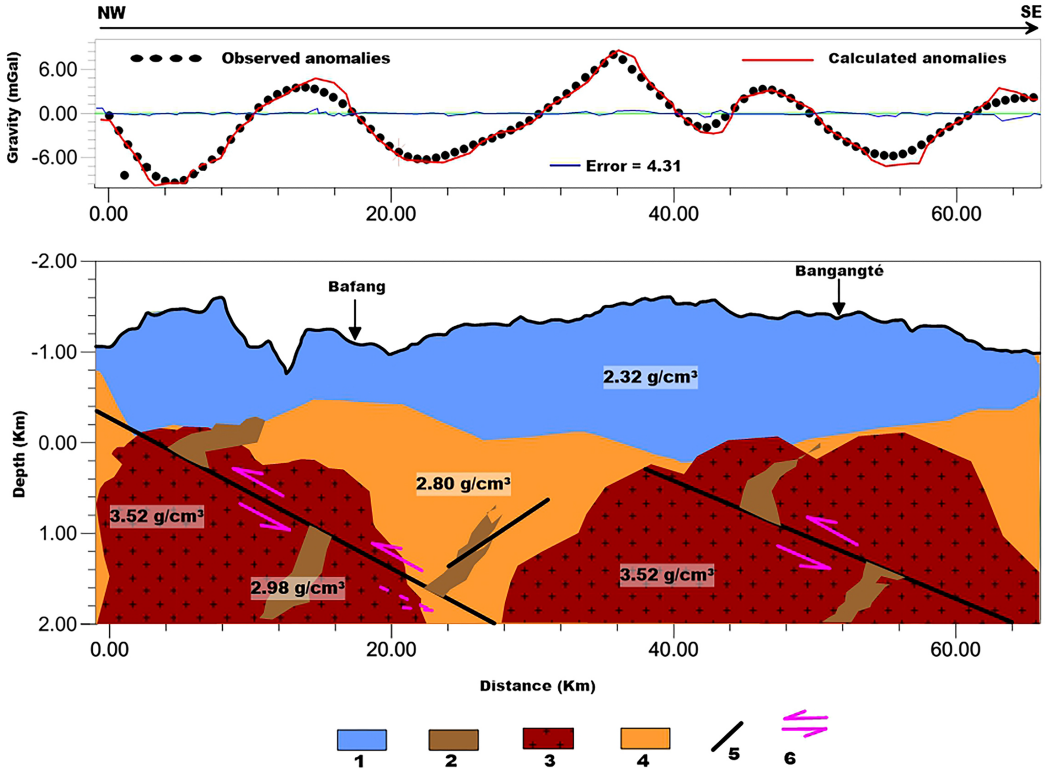

Figure 12. 2.5*D* model of profile P1 (1: Volcanic formations; 2: Dykes; 3: Granitic intrusions; 4: Gneissic bedrock; 5: Faults; 6: Kinematics).

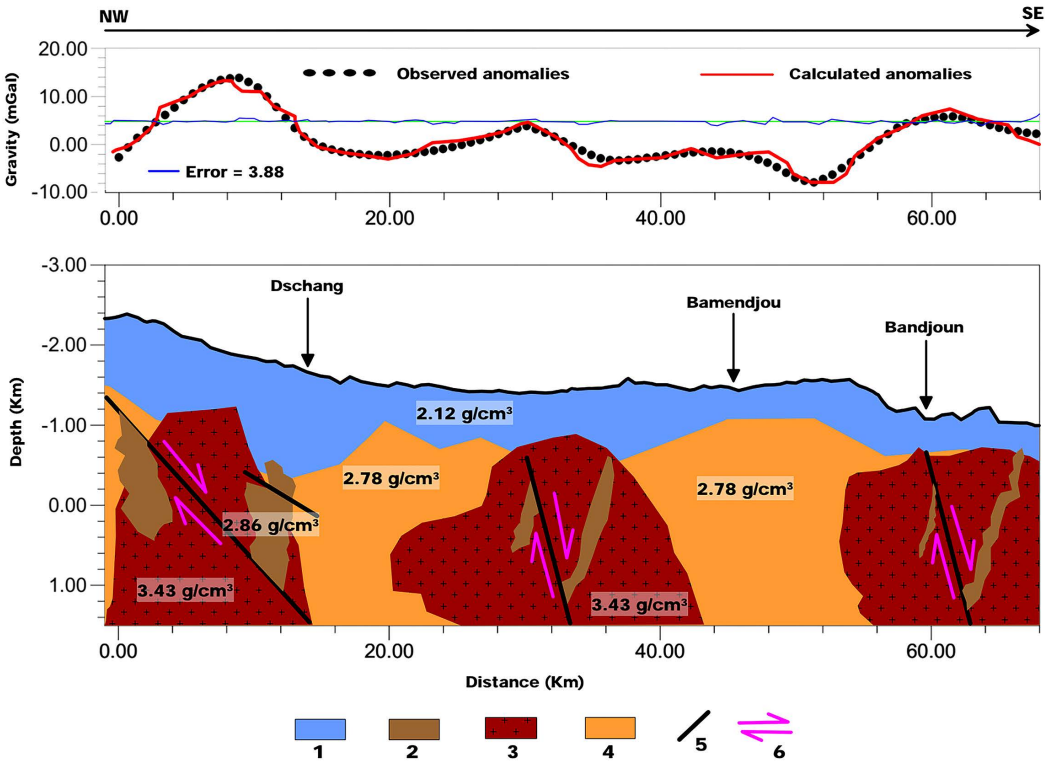

Figure 13. 2.5*D* model of the *P*2 profile (1: Volcanic formations; 2: Dykes; 3: Granitic intrusions; 4: Gneissic bedrock; 5: Faults; 6: Kinematics).

These models also reveal the substantial presence of volcanic formations overlying the granite-gneiss bedrock, with a maximum thickness of 1.8 km observed between Bafang and Bangangté (**Figure 12**) and a minimum thickness of 400 m in the vicinity of Bandjoun and Bamendjou (**Figure 13**). In these models, the major faults interpreted have no visible ends, showing their continuity at depth and outside the study area. The dextral or sinistral kinematics previously interpreted are also highlighted in these models. The dykes associated with these fault zones may constitute traps for valuable minerals such as Bangam and Fongo-Tongo bauxite (Mathieu et al., 2012; Sojien et al., 2018) already highlighted in the study area, and may also be of great interest for mineral exploration projects.

6. Conclusion

The aim of this study, based on the processing and interpretation of gravity data, was to provide basic information to facilitate the better understanding of the litho-structural beneath the Bamiléké Plateau that could be used for hydrogeological and mining investigation projects. The methodological approach used was to begin the study with geological field observations. As the structures of interest are near-surface, a regional-residual separation approach was applied to the Bouguer anomaly data, using the upward continuation separation method coupled with spectral analysis. The residual obtained highlights anomalies lying between the surface and an average maximum depth of 4 km. A set of processing steps was then applied to the residual grid (vertical derivative, analytical signal or SA and categorization of gravity signatures). Analysis of the vertical derivative map revealed a structural pattern corresponding to a set of dextral or sinistral strike-slip faults oriented N85E (ENE-WSW) to N95E (ESE-WNW) that affected the basement of the study area. The advent of this tectonics was accompanied by the development of a network of dykes in the study area. Analysis of the analytical signal map revealed anomalies corresponding to zones of granitic intrusions whose orientation (E-W to NNW-SSE) corroborates that described in numerous previous studies. The categorization of gravity signatures has made it possible to define the contours of lithological formations, and their association with previous analyses has led to the development of a synthetic geological model. The fault zones highlighted in the latter model are ideal areas for hydrogeological investigations, while the various dykes interpreted as corresponding to zones of late magmatic fluid upwelling are potential targets for mining exploration. In order to understand the vertical architecture of the geological structures and formations in the study area, 2.5D inversion modeling of two gravity profiles, $P1$ and $P2$, was carried out. The geological sections obtained show the influence of granitic intrusions in the geological system of the study area, as well as the structural control associated with the various dyke intrusions. The models obtained can be also used as basic documents for hydrogeological and mining investigations of the Bamiléké Plateau.

At present, 3D density inversion (regularization) is mature, and it is recommended to use this method constrained by 2.5D results to study the underground

density distribution. The 3*D* density results provide a better representation of the underground structure that may constitute the next paper projet.

Acknowledgement

Gravimetry anomaly grid data (Bouguer anomalies) are from the Earth Gravitational Model (EGM2008) released by the National Geospatial-Intelligence Agency (NGA). The authors are grateful to the Bureau Gravimétrique International (BGI)/International Association of Geodesy for their kind collaboration by providing EGM2008 data used in this paper.

Data Availability Statement

The data that support the findings of this study are available from the corresponding author upon reasonable request.

Conflicts of Interest

The authors declare that they have no known competing financial interests or personal relationships that could have appeared to influence the work reported in this paper.

References

Abate Essi, J. M., Marcel, J., Diab, D. A., Yene Atangana, J. Q., Abossolo Angue, M., & Mvondo Ondoa, J. (2019). Gravity Modeling of the Au-U Mineralized Crust at the North-Central Cameroon Illustrating Crustal Permeability. *Natural Resources Research, 29,* 473-497. https://doi.org/10.1007/s11053-019-09506-4

Abate Essi, J. M., Marcel, J., Yene Atangana, J. Q., Ahmad, A. D., Fita Dassou, E., Mbossi, E. F. et al. (2017). Interpretation of Gravity Data Derived from the Earth Gravitational Model EGM2008 in the Center-North Cameroon: Structural and Mining Implications. *Arabian Journal of Geosciences, 10,* 130-132. https://doi.org/10.1007/s12517-017-2919-y

Abate Essi, J. M., Njandjock Nouck, P., Sanda, O., & Manguelle Dicoum, E (2018). Validation of Gravity Data from the Geopotential Field Model for Subsurface Investigation of the Cameroon Volcanic Line (Western Africa). *Earth, Planets and Space, 70,* Article No. 42. https://doi.org/10.1186/s40623-018-0812-x

Abdelsalam, M. G., Liégeois, J., & Stern, R. J. (2002). The Saharan Metacraton. *Journal of African Earth Sciences, 34,* 119-136. https://doi.org/10.1016/s0899-5362(02)00013-1

Achu Megnemo, L., Kwékam, M., Fozing, E. M., Tcheumenak Kouémo, J., Efon Awoum Awoum, J., Choumele Kana, S. C., Sobze Yemdji, R. B., Kamgang Tchuifong, A. B., & Azemekeu Folefack, L. (2021). Field Observations and Microstructural Evidences of Syntectonic Emplacement of the Ngwi Granitic Plutons (Central Cameroon Domain). *Arabian Journal of Geosciences, 14,* Article No. 1497.

Almeida, F. F. M., Hasui, Y., de Brito Neves, B. B., & Fuck, R. A. (1981). Brazilian structural provinces: An introduction. *Earth-Science Reviews, 17,* 1-29. https://doi.org/10.1016/0012-8252(81)90003-9

Amante, C., & Eakins, B. (2008). *ETOPO1 1arc-Minute Global Relief Model: Procedures, Data Sources and Analysis.* NOAA Technical Memorandum.

Arsène, M., Hervé, G. D., Theophile, N. M., Mouhamed, N. N., & Igor, O. A. O. U. (2019). 2.5*D* Modelling of Aeromagnetic Data and Their Mining Implications over the Ngaoundere Area (Adamawa Province, Cameroon). *International Journal of Geosciences, 10,* 173-192. https://doi.org/10.4236/ijg.2019.102011

Balmino, G., Vales, N., Bonvalot, S., & Briais, A. (2011). Spherical Harmonic Modelling to Ultra-High Degree of Bouguer and Isostatic Anomalies. *Journal of Geodesy, 86,* 499-520. https://doi.org/10.1007/s00190-011-0533-4

Blakely, R. J., & Simpson, R. W. (1986). Rapprochement des bords des organismes à partir de la source des anomalies magnétiques et gravimétriques. *GEOPHYSICS, 51,* 1494-1498. https://doi.org/10.1190/1.1442197

Blandine, K. T. A., Jules, T. K., Martial, F. E., Ludovic, A. M., Julios, E. A., Robinson, S. B. et al. (2022). Geological Mapping and Structural Interpretation of the Dschang-Santchou-Escarpment (West, Cameroon), Using Landsat 8 OLI/TIRS Sensors/SRTM and Field Observations. *Geological Journal, 58,* 1111-1130. https://doi.org/10.1002/gj.4646

Brito Neves, B. B., Van Schmus, W. R., & Fetter, A. (2002). North-Wetern Africa-North-Eastern Brazil. Major Tectonic Links and Correlation Problems. *Journal of African Earth Sciences, 34,* 275-278. https://doi.org/10.1016/s0899-5362(02)00025-8

Cordani, U. G., D'Agrella-Filho, M. S., Brito-Neves, B. B., & Trindade, R. I. F. (2003). Tearing up Rodinia: The Neoproterozoic Palaeogeography of South American Cratonic Fragments. *Terra Nova, 15,* 350-359. https://doi.org/10.1046/j.1365-3121.2003.00506.x

Davison, I., & Dos Santos, R. A. (1989). Tectonic Evolution of the Sergipano Fold Belt, NE Brazil, during the Brasiliano Orogeny. *Precambrian Research, 45,* 319-342. https://doi.org/10.1016/0301-9268(89)90068-5

Djouka-Fonkwé, M. L., Schulz, B., Schüssler, U., Tchouankoué, J., & Nzolang, C. (2008). Geochemistry of the Bafoussam Pan-African I- and S-Type Granitoids in Western Cameroon. *Journal of African Earth Sciences, 50,* 148-167. https://doi.org/10.1016/j.jafrearsci.2007.09.015

Dumort, J. C. (1968). *Carte géologique de la reconnaissance de la république fédérale du Cameroun.* DEFORD.

Emishaw, L., Laó-Dávila, D. A., Abdelsalam, M. G., Atekwana, E. A., & Gao, S. S. (2017). Evolution of the Broadly Rifted Zone in Southern Ethiopia through Gravitational Collapse and Extension of Dynamic Topography. *Tectonophysics, 699,* 213-226. https://doi.org/10.1016/j.tecto.2016.12.009

Fofie, K. A. D., Koumetio, F., Victor Kenfack, J., & Yemele, D. (2019). Lineament Characteristics Using Gravity Data in the Garoua Zone, North Cameroon: Natural Risks Implications. *Earth and Planetary Physics, 3,* 33-44. https://doi.org/10.26464/epp2019009

Fosso, J., Ménard, J., Bardintzeff, J., Wandji, P., Tchoua, F. M., & Bellon, H. (2005). Les laves du mont Bangou: Une première manifestation volcanique éocène, à affinité transitionnelle, de la Ligne du Cameroun. *Comptes Rendus. Géoscience, 337,* 315-325. https://doi.org/10.1016/j.crte.2004.10.014

Fozing, E. M., Kwékam, M., Tcheumenak Kouémo, J., Njanko, T., & Njonfang, E. (2021). Kinematic Analysis of the Dschang Granitic Pluton (West-Cameroon): Implications to the Pan-African Deformation of the Central African Fold Belt in Cameroon during the Post-Collisional History of Western Gondwana. *Precambrian Research, 359,* Article ID: 106231. https://doi.org/10.1016/j.precamres.2021.106231

Fozing, E. M., Mengou, A. C., Njanko, T., Téfo Fokoua, A., Tiseh, I. K., Kwékam, M. et al.

(2019). Emplacement of the Dschang Granitic Pluton (West-Cameroon): Constraints from Microstructures and Magnetic Fabrics. *Journal of African Earth Sciences, 156,* 144-157. https://doi.org/10.1016/j.jafrearsci.2019.05.007

Fullea, J., Fernàndez, M., & Zeyen, H. (2008). FA2BOUG—A FORTRAN 90 Code to Compute Bouguer Gravity Anomalies from Gridded Free-Air Anomalies: Application to the Atlantic-Mediterranean Transition Zone. *Computers & Geosciences, 34,* 1665-1681. https://doi.org/10.1016/j.cageo.2008.02.018

Halliday, A. N., Dickin, A. P., Fallick, A. E., & Fitton, J. G. (1988). Mantle Dynamics: A Nd, Sr, Pb and O Isotopic Study of the Cameroon Line Volcanic Chain. *Journal of Petrology, 29,* 181-211. https://doi.org/10.1093/petrology/29.1.181

Jacobsen, B. H. (1987). A Case for Upward Continuation as a Standard Separation Filter for Potential-Field Maps. *Geophysics, 52,* 390-398. https://doi.org/10.1190/1.1442378

Julios, E. A., Martial, F. E., Maurice, K., Jules, T. K., Cliff, C. K. S., & Ludovic, A. M. (2020). Structural Characterization of the Pan-African Ndieki Area in the Foumban-Bankim Shear Zone (West Cameroon): Constraints from Field Observations and Microstructures. *Arabian Journal of Geosciences, 13,* Article No. 831. https://doi.org/10.1007/s12517-020-05775-z

Kagou Dongmo, A., Nkouathio, D., Pouclet, A., Bardintzeff, J., Wandji, P., Nono, A. et al. (2010). The Discovery of Late Quaternary Basalt on Mount Bambouto: Implications for Recent Widespread Volcanic Activity in the Southern Cameroon Line. *Journal of African Earth Sciences, 57,* 96-108. https://doi.org/10.1016/j.jafrearsci.2009.07.015

Kenfack, J. V., Tadjou, J. M., Kamguia, J., Tabod, T. C., & Bekoa, A. (2011). Gravity Interpretation of the Cameroon Mountain (West Central Africa) Based on the New and Existing Data. *International Journal of Geosciences, 02,* 513-522. https://doi.org/10.4236/ijg.2011.24054

Koumetio, F., Njomo, D., Tabod, C. T., Noutchogwe, T. C., & Manguelle-Dicoum, E. (2012). Structural Interpretation of Gravity Anomalies from the Kribi-Edea Zone, South Cameroon: A Case Study. *Journal of Geophysics and Engineering, 9,* 664-673. https://doi.org/10.1088/1742-2132/9/6/664

Kpirgbéne, W., Li Zhen, C., & Marc, L. (2016). *Cartographie géologique par méthode magnétique aéroportée: Application à deux zones de la région de l'abitibi-témiscamingue.* Ph.D. Thesis, Université du Québec.

Kuepouo, G., Tchouankoue, J. P., Nagao, T., & Sato, H. (2006). Transitional Tholeiitic Basalts in the Tertiary Bana Volcano–plutonic Complex, Cameroon Line. *Journal of African Earth Sciences, 45,* 318-332. https://doi.org/10.1016/j.jafrearsci.2006.03.005

Kwékam, M., Affaton, P., Bruguier, O., Liégeois, J., Hartmann, G., & Njonfang, E. (2013). The Pan-African Kekem Gabbro-Norite (West-Cameroon), U-Pb Zircon Age, Geochemistry and Sr-Nd Isotopes: Geodynamical Implication for the Evolution of the Central African Fold Belt. *Journal of African Earth Sciences, 84,* 70-88. https://doi.org/10.1016/j.jafrearsci.2013.03.010

Kwékam, M., Dunkl, I., Fozing, E. M., Hartmann, G., Njanko, T., Tcheumenak, K. J. et al. (2020a). Syn-kinematic Ferroan High-K I-Type Granites from Dschang in Southwestern Cameroon: U–pb Age, Geochemistry and Implications for Crustal Growth in the Late Pan-African Orogeny. *Geological Society, London, Special Publications, 502,* 191-213. https://doi.org/10.1144/sp502-2019-19

Kwékam, M., Dunkl, I., Fozing, E. M., Hartmann, G., Njanko, T., Tcheumenak, K. J. et al. (2021). Syn-kinematic Ferroan High-K I-Type Granites from Dschang in Southwestern Cameroon: U–pb Age, Geochemistry and Implications for Crustal Growth in the Late Pan-African Orogeny. *Geological Society, London, Special Publications, 502,* 191-213.

https://doi.org/10.1144/sp502-2019-19

Kwékam, M., Hartmann, G., Njanko, T., Tcheumenak Kouémo, J., Fozing, E.M., Njonfang, E. (2015). Geochemical and Isotope Sr-Nd Character of Dschang Biotite Granite: Implications for the Pan-African Continental Crust Evolution in West-Cameroon (Central Africa). *Earth Science Research, 4,* 88-102. https://doi.org/10.5539/esr.v4n1p88

Kwékam, M., Liégeois, J., Njonfang, E., Affaton, P., Hartmann, G., & Tchoua, F. (2010). Nature, Origin and Significance of the Fomopéa Pan-African High-K Calc-Alkaline Plutonic Complex in the Central African Fold Belt (Cameroon). *Journal of African Earth Sciences, 57,* 79-95. https://doi.org/10.1016/j.jafrearsci.2009.07.012

Kwékam, M., Talla, V., Fozing, E. M., Tcheumenak Kouémo, J., Dunkl, I., & Njonfang, E. (2020b). The Pan-African High-K I-Type Granites from Batié Complex, West Cameroon: Age, Origin, and Tectonic Implications. *Frontiers in Earth Science, 8,* Article 363. https://doi.org/10.3389/feart.2020.00363

Liégeois, J. P., Latouche, L., Boughrara, M., Navez, J., & Guiraud, M. (2003). The LATEA Metacraton (Central Hoggar, Tuareg Shield, Algeria): Behaviour of an Old Passive Margin during the Pan-African Orogeny. *Journal of African Earth Sciences, 37,* 161-190. https://doi.org/10.1016/j.jafrearsci.2003.05.004

Liégeois, J., Abdelsalam, M. G., Ennih, N., & Ouabadi, A. (2013). Metacraton: Nature, Genesis and Behavior. *Gondwana Research, 23,* 220-237. https://doi.org/10.1016/j.gr.2012.02.016

Marzoli, A., Piccirillo, E. M., Renne, P. R., Bellieni, G., Iacumin, M., Nyobe, J. B. et al. (2000). The Cameroon Volcanic Line Revisited: Petrogenesis of Continental Basaltic Magmas from Lithospheric and Asthenospheric Mantle Sources. *Journal of Petrology, 41,* 87-109. https://doi.org/10.1093/petrology/41.1.87

Mathieu, M. N., Paul, T., & Martin, Y. (2012). Multi-Scale Organization of the Doumbouo-Fokoué Bauxites Ore Deposits (west Cameroon): Implication to the Landscape Lowering. *Open Journal of Geology, 2,* 14-24. https://doi.org/10.4236/ojg.2012.21002

Maurice, Z. E. O., Arsène, M., Moustapha, N. N. M., Alain, Z. A., & Herve, G. D. (2023). Mapping Gold Mineralization Targets Using Geological Field and Magnetic Ground Data in the Yopa Area, Adamawa-Cameroon. *Pure and Applied Geophysics, 180,* 2257-2273. https://doi.org/10.1007/s00024-023-03259-1

Mounir, A., Ahmed, M., & Mustapha, M. (2012). Contribution of the Airborne Aeromagnetic Mapping to the Structural Identification of the Aquifer System of the Oasis' Springs of Figuig, Morocco. *Bulletin de l'Institut Scientifique, Rabat, section Sciences de la Terre, 34,* 29-40.

Ndam Njikam, M. M., Arsène, M., Alain, Z. A., Raouf, A., & Demianus, N. A. (2022). Study of the Geothermal Potential of the Locality of Kaladi and Its Surroundings (Adamawa-Cameroon) from the Frequency Processing of Magnetic Data. *International Journal of Geosciences, 13,* 1024-1039. https://doi.org/10.4236/ijg.2022.1311052

Ndam Njikam, M. M., Meying, A., Zanga Amougou, A., & Ngon Ngon, G. F. (2023). Mapping Transpressional and Transtensional Relay Zones by Coupling Geological and Geophysical Field Data: The Case of the Central Cameroon Shear Zone in the Mbere Administrative Division of the Adamawa Region in Cameroon. *Journal of African Earth Sciences, 199,* Article ID: 104816. https://doi.org/10.1016/j.jafrearsci.2022.104816

Ndikum, E. N., Koumetio, F., Kenfack, V. J., & Tabod, C. T. (2019). Gravity Study of the Douala Sub-Basin (Cameroon) Using Euler 3D Deconvolution, Source Edge Detection (SED) and Special Function Analysis. *SN Applied Sciences, 1,* Article No. 1200. https://doi.org/10.1007/s42452-019-1176-y

Ndikum, E. N., Tabod, C. T., Koumetio, F., Tatchum, N. C., & Victor, K. J. (2017). Evidence of Some Major Structures Underlying the Douala Sedimentary Sub-Basin: West African Coastal Basin. *Journal of Geoscience and Environment Protection, 5,* 161-172. https://doi.org/10.4236/gep.2017.57013

Ngako, V. (1999). *Les Déformations continentales panafricaines en Afrique Centrale. Résultat d'un poinçonnement de type himalayen.* Master's Thesis, University of Yaoundé, I.

Ngako, V., Affaton, P., & Njonfang, E. (2008). Pan-African Tectonics in Northwestern Cameroon: Implication for the History of Western Gondwana. *Gondwana Research, 14,* 509-522. https://doi.org/10.1016/j.gr.2008.02.002

Ngako, V., Affaton, P., Nnange, J. M., & Njanko, T. (2003). Pan-African Tectonic Evolution in Central and Southern Cameroon: Transpression and Transtension during Sinistral Shear Movements. *Journal of African Earth Sciences, 36,* 207-214. https://doi.org/10.1016/s0899-5362(03)00023-x

Ngnotué, T., Nzenti, J. P., Barbey, P., & Tchoua, F. M. (2000). The Ntui-Betamba High-Grade Gneisses: A Northward Extension of the Pan-African Yaoundé Gneisses in Cameroon. *Journal of African Earth Sciences, 31,* 369-381. https://doi.org/10.1016/s0899-5362(00)00094-4

Ngongang Tchikankou, N. L., Tcheumenak Kouémo, J., Tchuimegnie Ngongang, N. B., Noudiédié Kamgang, J. A., Kwekam, M., & Kamgang, P. (2020). The NE-SW Trending Fotouni and Fangam Basalt Cones: Evidence of Tectonic Control on Their Emplacement. *European Journal of Environment and Earth Sciences, 1,* 1-6. https://doi.org/10.24018/ejgeo.2020.1.5.70

Nguiessi Tchankam, C, Nzentui, J., Nsifa, E. N., Tempier, P., & Tchoua, F. (1997). Les granitoïdes calco-alcalins, syn-cisaillement de Bandja dans la chaîne panafricaine nord-équatoriale au Cameroun. *Comptes Rendus de l'Académie des Sciences—Series IIA—Earth and Planetary Science, 325,* 95-101. https://doi.org/10.1016/s1251-8050(97)83969-9

Njanko, T., Gountié Dedzo, M., Tamen, J., Bella Nke, E. B., Kadji Kouémo, O. S., Fozing, E. M. et al. (2020). Emplacement of the Zindeng Phonolitic Lava Flow (West-Cameroon) in the Cameroon Volcanic Line: Constraints from the Anisotropy of Magnetic Susceptibility (AMS). *Journal of African Earth Sciences, 162,* Article ID: 103728. https://doi.org/10.1016/j.jafrearsci.2019.103728

Njanko, T., Nédélec, A., & Affaton, P. (2006). Synkinematic High-K Calc-Alkaline Plutons Associated with the Pan-African Central Cameroon Shear Zone (w-Tibati Area): Petrology and Geodynamic Significance. *Journal of African Earth Sciences, 44,* 494-510. https://doi.org/10.1016/j.jafrearsci.2005.11.016

Njanko, T., Nédélec, A., Kwékam, M., Siqueira, R., & Esteban, L. (2010). Emplacement and Deformation of the Fomopéa Pluton: Implication for the Pan-African History of Western Cameroon. *Journal of Structural Geology, 32,* 306-320. https://doi.org/10.1016/j.jsg.2009.12.007

Njiekak, G., Dörr, W., Tchouankoué, J., & Zulauf, G. (2008). U-Pb Zircon and Microfabric Data of (Meta) Granitoids of Western Cameroon: Constraints on the Timing of Pluton Emplacement and Deformation in the Pan-African Belt of Central Africa. *Lithos, 102,* 460-477. https://doi.org/10.1016/j.lithos.2007.07.020

Njonfang, E., Ngako, V., Moreau, C., Affaton, P., & Diot, H. (2008). Restraining Bends in High Temperature Shear Zones: The "Central Cameroon Shear Zone", Central Africa. *Journal of African Earth Sciences, 52,* 9-20. https://doi.org/10.1016/j.jafrearsci.2008.03.002

Nkouathio, D. G., Kagou Dongmo, A., Bardintzeff, J. M., Wandji, P., Bellon, H., & Pouclet,

A. (2008). Evolution of Volcanism in Graben and Horst Structures along the Cenozoic Cameroon Line (Africa): Implications for Tectonic Evolution and Mantle Source Composition. *Mineralogy and Petrology, 94,* 287-303. https://doi.org/10.1007/s00710-008-0018-1

Nzenti, J. P. (1998). Neoproterozoic Alkaline Meta-Igneous Rocks from the Pan-African North Equatorial Fold Bel (Yaounde, Cameroon): Biotitites and Magnetite Rich Pyroxenites. *Journal of African Earth Sciences, 26,* 37-47. https://doi.org/10.1016/s0899-5362(97)00135-8

Nzenti, J. P., Barbey, P., & Tchoua, F. M. (1999). Evolution crustale au Cameroun: Eléments pour un modèle géodynamique de l'orogénèse néoprotérozoïque. *Géologie et environnements au Cameroun, collection GEOCA, 2,* 397-407.

O'leary, D. W., Friedman, J. D., & Pohn, H. A. (1976). Lineament, Linear, Lineation: Some Proposed New Standards for Old Terms. *Geological Society of America Bulletin, 87,* 1463. https://doi.org/10.1130/0016-7606(1976)87<1463:lllspn>2.0.co;2

Pal, P. C., Khurana, K. K., & Unnikrishnan, P. (1979). Two Examples of Spectral Approach to Source Depth Estimation in Gravity and Magnetics. *Pure and Applied Geophysics, 117,* 772-783. https://doi.org/10.1007/bf00879978

Pavlis, N. K., Holmes, S. A., Kenyon, S. C., & Factor, J. K. (2008). An Earth Gravitational Model to Degree 2160: EGM2008. In *EGU General Assembly, Vienna* (pp.13-18).

Pavlis, N. K., Holmes, S. A., Kenyon, S. C., & Factor, J. K. (2012). The Development and Evaluation of the Earth Gravitational Model 2008 (EGM2008). *Journal of Geophysical Research: Solid Earth, 117,* B04406. https://doi.org/10.1029/2011jb008916

Penaye, J., Toteu, S. F., Van Schumus, W. R., & Nzenti, J. P. (1993) U-Pb and Sm-Nd Preliminary Geochronologic Data on the Yaoundé Series Cameroon: Reinterpretation of the Granulitic Rocks as Suture of a Collision in the "Centrafrican" Belt. *C.R. Academie des Science, Paris, 317,* 789-794.

Pouclet, A., Vidal, M., Doumnang, J., Vicat, J., & Tchameni, R. (2006). Neoproterozoic Crustal Evolution in Southern Chad: Pan-African Ocean Basin Closing, Arc Accretion and Late- To Post-Orogenic Granitic Intrusion. *Journal of African Earth Sciences, 44,* 543-560. https://doi.org/10.1016/j.jafrearsci.2005.11.019

Poudjom Djomani, Y. H., Nnange, J. M., Diament, M., Ebinger, C. J., & Fairhead, J. D. (1995). Effective Elastic Thickness and Crustal Thickness Variations in West Central Africa Inferred from Gravity Data. *Journal of Geophysical Research: Solid Earth, 100,* 22047-22070. https://doi.org/10.1029/95jb01149

Poudjom-Djomani, Y. H., Boukeke, D. B., Legeley-Padovani, A., Nnange, J. M., Ateba, B., Albouy, Y., & Fairhead, J. D. (1996). *Levés gravimétriques de reconnaissance du Cameroun.* ORSTOM.

Powell, M. J. D. (1965). A Method for Minimizing a Sum of Squares of Non-Linear Functions without Calculating Derivatives. *The Computer Journal, 7,* 303-307. https://doi.org/10.1093/comjnl/7.4.303

Reeves, C. (2005). *Aeromagnetic Surveys: Principles, Practice and Interpretation* (p. 155). Earth-Works.

Saada, S. A. (2016). Edge Detection and Depth Estimation of Galala El Bahariya Plateau, Eastern Desert-Egypt, from Aeromagnetic Data. *Geomechanics and Geophysics for Geo-Energy and Geo-Resources, 2,* 25-41. https://doi.org/10.1007/s40948-015-0019-6

Sato, H., Aramaki, S., Kusakabe, M., Hirabayashi, J., Sano, Y., Nojiri, Y. et al. (1990). Geochemical Difference of Basalts between Polygenetic and Monogenetic Volcanoes in the Central Part of the Cameroon Volcanic Line. *Geochemical Journal, 24,* 357-370.

https://doi.org/10.2343/geochemj.24.357

Shuey, R. T., & Pasquale, A. S. (1973). End Corrections in Magnetic Profile Interpretation. *Geophysics, 38,* 507-512. https://doi.org/10.1190/1.1440356

Sobze Yemdji, B. R., Kouémo, J. T., Fozing, E. M., Megnemo, L. A., Awoum, J. E., Tchuifong, A. B. K. et al. (2023). Kinematic Evolution of the Nyakong-Manyi Shear Zone (Adamawa, Cameroon): Constraints from Field Observations and Microstructures, and Implication for Metamorphic P-T-T Estimation. *Journal of Earth Science, 34,* 1465-1487. https://doi.org/10.1007/s12583-023-1816-4

Soesilo, I., & Hoppin, R. A. (1986). Evaluation of Digitally Processed Landsat Imagery and SIR-A Imagery for Geological Analysis of West Java Region, Indonesia. In *Symposium on Remote Sensing for Resources Development and Environmental Management* (pp. 173-182). Publisher.

Sojien, T. M., Mamdem, E. L. T., Wouatong, A. S. L., & Bitom, D. L. (2018). Mineralogical, Geochemical and Distribution Study of Bauxites in the Locality of Bangam and Environs (west Cameroon). *Earth Science Research, 7,* 117-130. https://doi.org/10.5539/esr.v7n1p117

Tagne-Kamga, G. (2003). Petrogenesis of the Neoproterozoic Ngondo Plutonic Complex (Cameroon, West Central Africa): A Case of Late-Collisional Ferro-Potassic Magmatism. *Journal of African Earth Sciences, 36,* 149-171. https://doi.org/10.1016/s0899-5362(03)00043-5

Talwani, M., & Heirtzler, J. (1964). Computation of Magnetic Anomalies Caused by Two-Dimensional Bodies of Arbitrary Shape. In G. A. Parks (Ed.), *Computers in the Mineral Industries, Part 1* (pp. 464-480). Stanford University Publications.

Talwani, M., Worzel, J. L., & Landisman, M. (1959). Rapid Gravity Computations for Two-Dimensional Bodies with Application to the Mendocino Submarine Fracture Zone. *Journal of Geophysical Research, 64,* 49-59. https://doi.org/10.1029/jz064i001p00049

Tanko Njiosseu, E. L., Nzenti, J., Njanko, T., Kapajika, B., & Nédélec, A. (2005). New Upb Zircon Ages from Tonga (Cameroon): Coexisting Eburnean-transamazonian (2.1 Ga) and Pan-African (0.6 Ga) Imprints. *Comptes Rendus. Géoscience, 337,* 551-562. https://doi.org/10.1016/j.crte.2005.02.005

Tchameni, R., Pouclet, A., Penaye, J., Ganwa, A. A., & Toteu, S. F. (2006). Petrography and Geochemistry of the Ngaoundéré Pan-African Granitoids in Central North Cameroon: Implications for Their Sources and Geological Setting. *Journal of African Earth Sciences, 44,* 511-529. https://doi.org/10.1016/j.jafrearsci.2005.11.017

Tchaptchet Tchato, D., Tchaptchet Schulz, B., & Nzenti, J. (2009). Electron Microprobe Dating and Thermobarometry of Neoproterozoic Metamorphic Events in the Kekem Area, Central African Fold Belt of Cameroon. *Neues Jahrbuch für Mineralogie—Abhandlungen, 186,* 95-109. https://doi.org/10.1127/0077-7757/2009/0140

Tcheumenak Kouémo, J. (2018). *Pétrographie, géochimie et structure de la zone de cisaillement de Fotouni-Kékem (Ouest-Cameroun): Implications géodynamiques sur le Cisaillement Centre Camerounais.* Ph.D. Thesis, Université de Dschang.

Tcheumenak Kouémo, J., Fozing, E. M., Zagalo Al-hadj, H., Noudiédié Kamgang, J. A., Kwékam, M., & Njonfang, E. (2023). Structural and Petrographic Characterization of the Fotouni-Kekem Shear Zone: Implication for P-T-t Regional Metamorphism and Mylonitic Evolutions along the Central Cameroon Shear Zone. *Arabian Journal of Geosciences, 16,* Article No. 38.

Tcheumenak Kouémo, J., Njanko, T., Kwékam, M., Naba, S., Bella Nké, B. E., Yakeu Sandjo, A. F. et al. (2014). Kinematic Evolution of the Fodjomekwet-Fotouni Shear Zone

(west-Cameroon): Implications for Emplacement of the Fomopéa and Bandja Plutons. *Journal of African Earth Sciences, 99,* 261-275. https://doi.org/10.1016/j.jafrearsci.2014.07.018

Tcheumenak Kouemo, J., Sobze Yemdji, B. R., Fozing, E. M., Tepi Yemele, B. R., Azefack Mbounou, R. L., & Kwekam, M. (2024). Petrogaphic and Structural Analyses of High-Grade Amphibolites from Fotouni-Kékem and Nyakong-Manyi Shear Zones: Implications for the Geodynamic Significance of the Central Cameroon Shear Zone. *Environmental Earth Sciences, 83,* Article No. 523. https://doi.org/10.1007/s12665-024-11811-y

Tchouankoué, J. P. (1992). *La syénite de Bangangté: Un complexe Panafricain à caractères intermédiaires: Pétrologie et Géochimie.* Master's Thesis, Université Yaoundé.

Tchouankoue, J. P., Simeni Wambo, N. A., Kagou Dongmo, A., & Li, X. (2014). 40ar/39ar Dating of Basaltic Dykes Swarm in Western Cameroon: Evidence of Late Paleozoic and Mesozoic Magmatism in the Corridor of the Cameroon Line. *Journal of African Earth Sciences, 93,* 14-22. https://doi.org/10.1016/j.jafrearsci.2014.01.006

Tchouankoue, J. P., Simeni Wambo, N. A., Kagou Dongmo, A., & Wörner, G. (2012). Petrology, Geochemistry, and Geodynamic Implications of Basaltic Dyke Swarms from the Southern Continental Part of the Cameroon Volcanic Line, Central Africa. *The Open Geology Journal, 6,* 72-84. https://doi.org/10.2174/1874262901206010072

Tchuimegnie Ngongang, N. B., Kamgang, P., Chazot, G., Agranier, A., Bellon, H., & Nonnotte, P. (2015). Age, Geochemical Characteristics and Petrogenesis of Cenozoic Intraplate Alkaline Volcanic Rocks in the Bafang Region, West Cameroon. *Journal of African Earth Sciences, 102,* 218-232. https://doi.org/10.1016/j.jafrearsci.2014.10.011

Toteu, S. F., Deloule, E., Penaye, J., & Tchameni, R. (2004). Preliminary U-Pb Ionic Microprobe Data on Zircons from Poli and Lom Volcano-Sedimentary Basins (Cameroon): Evidence for Late-Mesoproterozoic (1100-950Ma) Magmatic Activity in the Central African Fold Belt. In *The IGCP-470 Second Annual Field Conference*.

Toteu, S. F., Penaye, J., Deschamps, Y., Maldan, F., Nyama Atibagoua, B., Bouyou Houketchang, M., Sep Nlomgan, J. P., & Mbola Nzana, S. P. (2008). Géologie et resources min-erals du Cameroun. In *33rd International Geological Congres*.

Toteu, S. F., Van Schmus, W. R., Penaye, J., & Michard, A. (2001). New U-Pb and Sm-Nd Data from North-Central Cameroon and Its Bearing on the Pre-Pan African History of Central Africa. *Precambrian Research, 108,* 45-73. https://doi.org/10.1016/s0301-9268(00)00149-2

Wandji, P., Tchokona Seuwui, D., Bardintzeff, J., Bellon, H., & Platevoet, B. (2008). Rhyolites of the Mbépit Massif in the Cameroon Volcanic Line: An Early Extrusive Volcanic Episode of Eocene Age. *Mineralogy and Petrology, 94,* 271-286. https://doi.org/10.1007/s00710-008-0013-6

Won, I. J., & Bevis, M. (1987). Computing the Gravitational and Magnetic Anomalies Due to a Polygon: Algorithms and Fortran Subroutines. *Geophysics, 52,* 232-238. https://doi.org/10.1190/1.1442298

Yatabe, S., & Howarth, P. H. (1984). Lineament Enhancernent and Interpretation in Northem Ontario from Airborne, Multispectral Scanner Data. In *Proceedings of the International Symposium on Remote Sensing, 3D Thematic Conference, Remote Sensing for Exploration Geology* (pp. 1-8).

Zangmo Tefogoum, G., Nkouathio, D. G., Kagou Dongmo, A., & Gountié Dedzo, M. (2019). Typology of Geotouristic Assets along the South Continental Branch of the Cameroon Volcanic Line: Case of the Mount Bambouto's Caldera. *International Journal of Geoheritage and Parks, 7,* 111-128. https://doi.org/10.1016/j.ijgeop.2019.06.003

Zelalem, D., Mickus, K., Bridges, D., Abdelsalam, M. G., & Atekwana, E. (2018). Upper Lithospheric Structure of the Dobi Graben, Afar Depression from Magnetics and Gravity Data. *Journal of African Earth Sciences, 147,* 136-151. https://doi.org/10.1016/j.jafrearsci.2018.06.012

Ziada Tabengo, M., Tassongwa, B., Tamen, J., Nkoumbou, C., Njanko, T., Asaah, A. N. E. et al. (2022). Petrology and Geochemistry of the Batchingou Anorthositic Suite Rocks (Bana Volcano-Plutonic Complex, Cameroon Volcanic Line): Inference on Their Origin and Relation with Host Granites. *Geological Journal, 57,* 4262-4284. https://doi.org/10.1002/gj.4543